Global and Planetary Change 206 (2021) 103634

Contents lists available at ScienceDirect

Global and Planetary Change

journal homepage: www.elsevier.com/locate/gloplacha

Dextral to sinistral coiling switch in planktic foraminifer *Morozovella* during the Early Eocene Climatic Optimum

Valeria Luciani [a,*], Roberta D'Onofrio [a], Gerald R. Dickens [b], Bridget S. Wade [c]

[a] Dipartimento di Fisica e Scienze della Terra, Ferrara University, via G. Saragat 1, 44121, Italy
[b] Department of Geology, Museum Building, Trinity College Dublin, College Green, Dublin 2, Ireland
[c] Department of Earth Sciences, University College London, Gower Street, London WC1E 6BT, United Kingdom

ARTICLE INFO

Editor: Fabienne Marret-Davies

Keywords:
Planktic foraminifera
Morozovella
Early Eocene Climatic Optimum
Coiling direction
Stable isotopes

ABSTRACT

Coiling direction is a basic characteristic of trochospiral planktic foraminifera. Modifications in the coiling direction within ancient planktic foraminiferal populations may reflect important changes in evolution or environment, yet they remain scarcely discussed. Here we investigate fluctuations in the coiling direction within *Morozovella* assemblages from sections that span the interval of peak Cenozoic warmth, the Early Eocene Climatic Optimum (EECO; ~53–49 million years ago, Ma), at Atlantic Ocean Drilling Program (ODP) sites 1051, 1258 and 1263. The surface-dwelling genus *Morozovella* is of particular interest because it dominated tropical-subtropical early Paleogene assemblages then suffered an abrupt and permanent decline in abundance and taxonomic diversity at the start of the EECO. At all ODP sites, morozovellids display a dominant dextral coiling preference during the interval preceding the EECO. However, all the *Morozovella* species at all sites modify their coiling from preferentially dextral to sinistral coiling within the EECO, <200 kyr after the K/X event (~52.8 Ma), providing a new biostratigraphic tool for correlation. We also document that before the major shift in morozovellid coiling, transient excursions to higher abundances of sinistral tests occurred in conjunction with negative carbon isotope excursions. Significantly, carbon isotope data reveal that sinistral morphotypes belonging to the same morphospecies typically have lower $\delta^{13}C$ values. The dominance of sinistral morphotypes, at the expense of dextral forms within the EECO, coupled with the lower $\delta^{13}C$ signatures of the former, suggests that the sinistral forms were less dependent on their photosymbiotic partnerships and thus able to adapt more readily to paleoceanographic change at the EECO. The observed sinistral and dextral coiling of morozovellids can be a genetically heritable characteristic that lies within cryptic speciation across multiple morphologically defined species. Alternatively the coiling changes were exclusively ecophenotypic responses whereby different species were able to preferentially adopt sinistral coiling in reaction to the changed conditions in the mixed-layer during the EECO. Previous interpretations of coiling flips in planktic foraminifera in the early Eocene, especially including morozovellids, have favoured a genetic explanation rather than an ecological response. Our present data cannot validate or disprove this idea, but should stimulate renewed thought on the matter.

1. Introduction

Evolutionary trends of planktic foraminifera and major modifications in their abundance often appear to correlate with significant changes in oceanography, although causal relationships remain uncertain (e.g., Schmidt et al., 2004; Wade and Pearson, 2008; Ezard et al., 2011; Fraass et al., 2015). The early Paleogene represents an important time to study such linkages due to global warmth and perturbations in the carbon cycle. Earth surface generally warmed from the late Paleocene through the start of the Early Eocene Climatic Optimum (EECO), a loosely defined interval between 53 and 49 million years ago (Ma) (Slotnick et al., 2012, 2015; Lauretano et al., 2016; Luciani et al., 2016; Westerhold et al., 2018; Hollis et al., 2019), when ocean temperatures reached their Cenozoic peak (e.g., Zachos et al., 2001, 2008; Bijl et al., 2009; Huber and Caballero, 2011; Hollis et al., 2012; Pross et al., 2012; Inglis et al., 2015). Indeed, recent estimation of global mean surface ocean temperature records average of ~27 °C, that is ~10 to ~16 °C warmer than pre-industrial temperatures (Inglis et al., 2020). Superimposed on the long-term thermal trend were several short-lived (~40–200 Kyr) events of excess warming (e.g., Lourens et al., 2005;

* Corresponding author.
E-mail addresses: valeria.luciani@unife.it (V. Luciani), dnfrrt@unife.it (R. D'Onofrio), dickensg@tcd.ie (G.R. Dickens), b.wade@ucl.ac.uk (B.S. Wade).

https://doi.org/10.1016/j.gloplacha.2021.103634
Received 17 February 2021; Received in revised form 27 August 2021; Accepted 27 August 2021
Available online 1 September 2021

Nicolo et al., 2007; Lauretano et al., 2016). Beyond rapid rises in ocean temperature, these "hyperthermals" (Thomas, 1998) share several key characteristics, most notably negative carbon isotope ($\delta^{13}C$) excursions (CIEs) and evidence for dissolution of deep-sea carbonate (e.g., Zachos et al., 2005; Leon-Rodriguez and Dickens, 2010). Several hyperthermals have been identified, beside the widely studied Paleocene Eocene Thermal Maximum (PETM, ~56 Ma), including the H-1 or ETM2 (~54 Ma), I-1 (~ 53.6 Ma), J (~53 Ma) and K/X or ETM3 events (~ 52.8 Ma) (Cramer et al., 2003; Lourens et al., 2005; Nicolo et al., 2007; Agnini et al., 2009; Stap et al., 2009, 2010a, 2010b; Zachos et al., 2010; Coccioni et al., 2012; D'Onofrio et al., 2014, 2016; Kirtland-Turner et al., 2014; Littler et al., 2014; Lauretano et al., 2015), with the J event initiating the EECO according to Slotnick et al. (2012, 2015), Lauretano et al. (2016) and Luciani et al. (2016).

Major turnovers within planktic foraminiferal assemblages occurred during the early Paleogene, which resulted in the diversification of some groups and species reductions for other groups (Norris, 1991; Schmidt et al., 2004; Pearson et al., 2006; Aze et al., 2011; Fraass et al., 2015). The symbiont-bearing surface-dweller genus *Morozovella* is of special interest, as this genus dominated planktic foraminiferal assemblages from tropical-subtropical regions in the early Paleogene (e.g., Boersma and Premoli Silva, 1983; Premoli Silva and Boersma, 1988). However, this genus markedly and permanently declinesd in relative abundance and taxonomic diversity at the beginning of the EECO (Pearson et al., 2006; Aze et al., 2011; Fraass et al., 2015; Luciani et al., 2016; Luciani et al., 2017a, 2017b; D'Onofrio et al., 2020). Moreover, at multiple sites (Fig. 1), this striking modification in morozovellids occurred rapidly and close in time to the CIE marking the J event (Luciani et al., 2016; Luciani et al., 2017a; D'Onofrio et al., 2020). The pronounced decrease in morozovellid abundance is accompanied by species reduction and by an increase in the relative abundance and diversity of the genus *Acarinina* (Aze et al., 2011; Pearson et al., 2006; Fraass et al., 2015; Luciani et al., 2016, 2017a, 2017b; D'Onofrio et al., 2020). Several potential stressors may explain the morozovellid crash, including some combination of algal photosymbiont inhibition (bleaching), a sustained increase in temperature, or an extended decrease in *p*H (Luciani et al., 2017a). The dramatic morozovellid decline at the start of the EECO presents a fascinating focal point for biological evolution but requires a more exhaustive documentation.

A basic characteristic of all trochospiral foraminifera, including

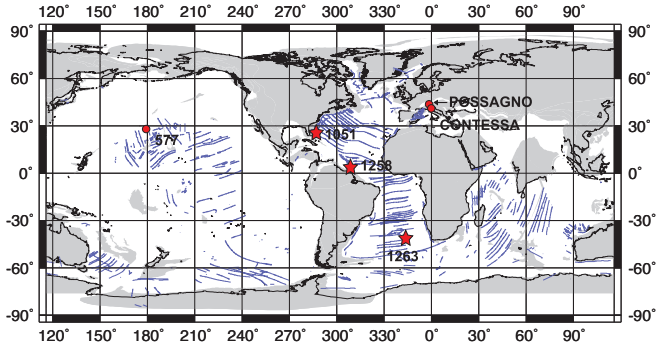

Fig. 1. Locations of the studied sites (red stars) during the early Eocene. Also shown are the positions for other successions (red circles) where quantitative planktic foraminiferal investigations show a major switch in genera (i.e., permanent decline in *Morozovella* and increase in *Acarinina* abundances) across the start of the EECO (Frontalini et al., 2016; Luciani et al., 2016, 2017a, 2017b). Base map is from http://www.odsn/de/services/paleomap.html with paleolatitudes modified for Sites 577, 1051 and 1263 according to www.paleolatitude.org model version 1.2 (Van Hinsbergen et al., 2015). Possagno paleolatitude is based on the http://www.odsn.de/odsn/services/paleomap/adv_map.html model since it is not yet available at http://www.odsn/de/services/paleomap.html. (For interpretation of the references to colour in this figure legend, the reader is referred to the web version of this article.)

Morozovella, is the coiling direction. This is the ability to grow their shells by adding chambers in a clockwise (dextral, DX hereafter) or counter-clockwise (sinistral, SN hereafter) direction, as observed in spiral-side view (Fig. 2). Although modifications in the coiling direction within Eocene planktic foraminiferal populations may reflect important changes in evolution or environment, they remain scarcely studied. Specifically, as further discussed below, such changes may relate to ecophenotypic adaption, when a single species changes morphology in response to variation in environmental parameters, such as temperature (e.g., Ericson et al., 1955; Ericson, 1959; Bandy, 1960), or when environmental conditions favor the more competitive morphological type, so it becomes the main component of the assemblages. Diverse types of coiling can also derive from genetic variance, when two almost identical morphotypes have different genetic signatures so they represent 'cryptic' species from a morphological point of view (e.g., Darling et al., 2004, 2006).

So, do various morozovellids display major flips in coiling through the dramatic changes in early Eocene oceanography, and if this is the case, how do these relate to the major modifications in abundance and diversity?

To answer to this question, we analyse here changes in the coiling direction of multiple species of *Morozovella* at the three widely separated locations from the Atlantic Ocean where the reduction in morozovellid abundance already has been documented: Ocean Drilling Program (ODP) sites 1051, 1258 and 1263 (Fig. 1). For the first time, modifications in *Morozovella* coiling direction are shown to correlate with established changes in temperature and carbon cycling, as expressed by stable isotope of bulk sediment. We demonstrate that significant changes in coiling direction occurred in multiple morphologically distinct species near the start of the EECO. In addition, we measured stable isotopes ($\delta^{13}C$ and $\delta^{18}O$) on DX and SN *Morozovella* to evaluate habitats and paleoecology within the water column through this time of critical paleoceanographic change.

2. Background: coiling direction in planktic foraminifera and its significance

Morphospecies of trochospiral planktic foraminifera can have populations with sub-equal proportions of right- and left-coiling tests, but also can have populations with a strong preference for either coiling direction. Distinct differences in the preferred coiling direction for a "species" have been observed in marine sediments across both space and time.

For the present-day ocean and late Neogene sediment, the relationship between the coiling ratio of a species and environmental parameters has been described quantitatively and utilized extensively, often to reconstruct paleoceanographic conditions (e.g., Ericson et al., 1955; Bandy, 1960, 1972; Saito, 1976; Bond et al., 1993; Xu et al., 1995; Renaud and Schmidt, 2003; Martinez et al., 2007; Billups et al., 2020). A well-known example is *Neogloboquadrina 'pachyderma'*, in which sinistrally coiled forms preferentially have a modern polar distribution while dextrally coiled forms extensively have a sub-polar distribution (e.g., Ericson et al., 1955; Bandy, 1960, 1972; Saito, 1976; Bond et al., 1993; Xu et al., 1995; Kucera and Kennett, 2002; Bauch et al., 2003; Renaud and Schmidt, 2003; Martinez et al., 2007). Traditionally, changes in preferred coiling at a location over time have been ascribed to ecophenotypic adaptation (Ericson, 1959; Ericson et al., 1955; Bandy, 1960). However, for *N. 'pachyderma'*, genetic signatures demonstrate that the SN and DX morphotypes actually represent separate species (Darling et al., 2004), with the latter named *Neogloboquadrina incompta* (Darling et al., 2006), as originally described by Cifelli (1961). The coiling direction in *N. 'pachyderma'* is, therefore, a genetic trait, heritable through time, rather than a morphological feature reflecting ecophenotypic variation (Darling et al., 2006). On the other hand, Darling et al. (2003) found that left- and right-coiled individuals within morphotypes of *Globorotalia truncatulinoides* Type II and *Globigerina bulloides* have the

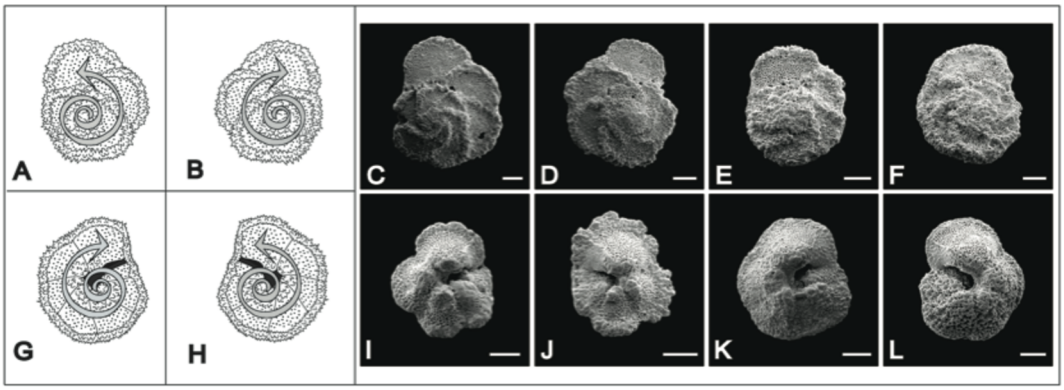

Fig. 2. Examples of SN and DX coiling within the same morphospecies of *Morozovella* from the early Eocene sediments of the Site 1051. A-B: cartoons showing spiral view of SN (A) and DX (B) coiled *Morozovella crater*. C-D: SN (C, sample 423.42 mbsf, Hole 1051A, 45X-4, 22-24 cm) and DX (D, Hole 1051A, 428.34 mbsf, 46X-X1, 4-6 cm) *Morozovella formosa. E*-F: SN (E, Hole 1051A, sample 405.22 mbsf, 43X-4, 122–124 cm) and DX *Morozovella aragonensis* (F, Hole 1051A, sample 427.99 mbsf, 45X−7, 29–31 cm). G-H: Cartoons of SN (G) and DX (H) coiled *Morozovella aragonensis* in umbilical view where chambers increase appears in the opposite direction with respect to the dorsal view. I-J: SN (I, Hole 1051A, sample 423.42 mbsf, 45X-4, 22–24 cm) and DX (J, Hole 1051A, 428.34 mbsf,46X-1,4–6 cm) *Morozovella marginodentata.* K-L: SN (K, Hole 1051A, sample 395.1 mbsf, 42 × 4, 70-72 cm) and DX (L, Hole 1051A, sample 432.5, 46X-3, 120–122 cm) *Morozovella crater*. Scale bar: 100 μm.

same genetic signatures. The co-occurrence of species that exhibit different coiling directions might suggest environmental controls on morphology. This supposition was confirmed by Ujiié and Asami (2014) who showed both SN and DX coiling morphotypes in genetically similar *G. truncatulinoides* Type II.

Interestingly, most cryptic species of recent planktic foraminifera clearly display ecological preferences for different water-masses (e.g., Ujiié et al., 2010; Morard et al., 2016). Adaptation to environmental change, therefore, may enable speciation of planktic foraminifera. For example, the two inversely coiled forms of *G. truncatulinoides* Type II, diverge in ecology with populations inhabiting different water masses. A niche partitioning between DX and SN *G. truncatulinoides* Type II suggests that these forms have the potential to genetically diverge from each other, similar to *Globigerinoides ruber*, which contains two sister genetic types in the Mediterranean Sea (Aurahs et al., 2009). It appears that chemical and physical parameters of water-masses provide sufficient separation for speciation, even in the absence of geographic barriers, thus inducing a sort of para-patric speciation. In this regards, Pearson and Penny (2021), examining the coiling fluctuations in genus *Pulleniatina* during the last ~6 Ma from the tropical west Pacific and Indian Oceans, showed significant differences in both carbon and oxygen isotopes of dextral and sinistral tests, implying a degree of ecological separation between populations. The authors suggested that major fluctuations in coiling ratio were caused by cryptic populations replacing one another in competitive sweeps.

From the considerations above, the meaning and mechanisms for switches in planktic foraminiferal coiling direction both in living and fossil forms still present open questions. Even assuming an ecophenotypic response, controversy surrounds the primary environmental parameter influencing coiling direction (e.g., Boltovoskoy and Wright, 1976; Khare et al., 2012 and reference therein). A plethora of alternative explanations can be offered, such as variations in seasonality, water depth, test size, differential predation, modification of water properties (e.g., temperature, productivity, salinity and density), possible asexual reproduction and even paleomagnetism (Scott, 1974; see review by Khare et al., 2012).

Sinistral and dextral coiling preferences have been recorded for some morphologically defined species from sediment sequences older than the late Neogene (e.g., Bolli, 1950, 1971; Caron, 1981; Malmgren, 1989; Pearson, 1993; Norris and Nishi, 2001; Hancock, 2005; Coccioni et al., 2016; Desmares et al., 2016; Grosheny et al., 2017). Hancock (2005) demonstrated a prominent coiling switch from DX to SN in the late Paleocene surface-dwelling planktic foraminifera *Igorina albeari* at three low latitude sites from the central Pacific ocean at ~59 Ma. The morphological change coincides with widespread dissolution throughout the central Pacific Ocean and with a positive $\delta^{13}C$ excursion that occurred near the base of the Paleocene Carbon Isotope Maximum (PCIM, Zachos et al., 2001). At one of the sites examined (Hole 865B), apparent cooling of the deep thermocline coincides with the switch to a sinistrally dominated population. However, stable isotopes from *I. albeari* specimens suggest that both SN and DX morphotypes occupied similar surface-water masses whatever genetically or ecologically driven. The coiling reversal was therefore ascribed to change in other ecological parameters such as feeding strategy for nutrient availability (Hancock, 2005). Whatever were the triggering mechanism, the recorded coiling shift provides an important biomarker in the Pacific Ocean sediment that marks the PCIM (Hancock, 2005).

Pearson (1993) documented the coiling preferences of members of the *Morozovella velascoensis* group, which is characterized by dominantly SN coiling and became extinct in the earliest Eocene. By contrast, members of the *Morozovella aequa* group, which include *M. subbotinae*, *M. gracilis*, *M. lensiformis* were characterized by dominantly DX coiling. However, according to Bolli (1950) and Luterbacher (1964), the *M. lensiformis* group, reversed its preferred direction of coiling from DX to SN at the extinction level of the *M. subbotinae.* The aforementioned changes in coiling direction have been related to evidence of genetic divergence (Pearson, 1993).

The formative work on coiling direction of early Paleogene planktic foraminifera (Norris and Nishi, 2001) focused on a condensed sediment section at ODP Site 865 in the equatorial Pacific. These authors highlighted a strong DX coiling preference for all *Morozovella* species in earliest Eocene assemblages, and, for *M. aragonensis*, a switch to a strong SN coiling preference within foraminiferal Zone E5. Norris and Nishi (2001) deduced that coiling patterns in Paleogene tropical planktic foraminifera did not result from environmental control but were instead heritable through time. However, Norris and Nishi (2001) and Pearson (1993) did not examine relationships to relative abundance and carbon cycle perturbations. The purpose of our present research is to focus on a restricted interval of the early Eocene when the *Morozovella* genus suffered a striking decline in abundance and in taxonomic diversity, and when possible switches in coiling direction of various *Morozovella* species can be compared to prominent changes in oceanography and global carbon cycling.

3. Selected locations: Atlantic ODP sites 1051, 1258 and 1263

The three sedimentary sections, from ODP Site 1051 (Blake Nose, NW Atlantic), ODP Site 1258 (Demerara Rise, equatorial Atlantic) and ODP Site 1263 (Walvis Ridge, SE Atlantic) (Fig. 1), were selected for this study because they record a major decline in morozovellid abundance. Additionally, at these sites, the lower Eocene interval has very good chronology, determined through calcareous nannofossil and planktic foraminiferal events, as well as detailed carbon isotope records (Site 1051: Norris et al., 1998; Mita, 2001; Cramer et al., 2003; Luciani and Giusberti, 2014; Luciani et al., 2016, 2017a; Site 1258: Shipboard Scientific Party, 2004; Sexton et al., 2006; Kirtland-Turner et al., 2014; Westerhold et al., 2012, 2017; D'Onofrio et al., 2020; Site 1263: Lourens et al., 2005; Westerhold et al., 2007, Stap et al., 2009, 2010a, 2010b; Lauretano et al., 2015, 2016; Luciani et al., 2016, 2017b).

The zonal scheme of Wade et al. (2011), which defines and dates bases (B) and tops (T) of key planktic foraminiferal species, was applied at the selected sites (Luciani et al., 2016, 2017a,b; D'Onofrio et al., 2020). However, as noted previously at other locations (Luciani and Giusberti, 2014; Luciani et al., 2016), a problem arises for the boundary between Zone E6 and Zone E7. This boundary is defined on the B of *Acarinina cuneicamerata* (Wade et al., 2011), which at multiple sites has been revealed to be diachronous. For example, at Site 1051, Site 1263, and the Possagno section of northern Italy, the B of *A. cuneicamerata* lies below T *Morozovella subbotinae*, but the latter marks the boundary between Zone E5 and Zone E6. Given the diachroneity of this datum, Luciani and Giusberti (2014) tentatively proposed the B *Astrorotalia* (*Planorotalites*) *palmerae,* which was recorded at Site 1258, as an alternative marker for the E6/E7 boundary. However, *A. palmerae* is absent at both sites 1051 and 1263, so Zone E6 and Subzone E7a are undifferentiated (Figs. 3-5) (Luciani et al., 2016; Luciani et al., 2017a, 2017b).

Site 1051 is located at 30° 03′ N, 76° 2′ W, but was positioned slightly further south during the early Eocene (Ogg and Bardot, 2001; Van Hinsbergen et al., 2015). The present water depth is 1992 m, and may have been similar or slightly shallower during the Paleocene and early Eocene as determined through benthic foraminiferal assemblages (1000–2000 m; Norris et al., 1998) or subsidence and sedimentation rate calculations (2200 m at ~50 Ma; Bohaty et al., 2009). The interval studied here is from 452 mbsf to 353 mbsf at Hole 1051A (the same as investigated by Luciani et al., 2016, 2017a). This succession has high sedimentation rate and good sediment recovery with the exception for a hiatus between C23n and C21r (Shipboard Scientific Party, 1998; Witkowski et al., 2020a).

Site 1258 is located at 9° 26′ N, 54° 44′ W, and 3192 m below sea level. The site lies on the northwest-facing slope of a small promontory of Demerara Rise (Shipboard Scientific party, 2004). During the early Eocene, the latitude was ~1° S and the water depth was ~3000 m (Shipboard Scientific Party, 2004). The Eocene interval is described as foraminiferal-nannofossil chalk, with samples averaging about ~60% $CaCO_3$ by weight; planktic foraminifera comprise about 10–25% by volume (Shipboard Scientific Party, 2004). Three holes (A, B, C) were drilled via the rotary coring method at Site 1258. Of interest to this study is Unit IIA, which spans from about 6 to 241 m below seafloor (mbsf), the same adopted by D'Onofrio et al. (2020). Even though recovered by the rotary method, cores across Unit IIA at the three holes at Site 1258 can be aligned through records of physical properties (Shipboard Scientific Party, 2004). Such alignment leads to a "revised meter composite depth" (rmcd) scale (Kirtland-Turner et al., 2014). From the stratigraphy and the spliced records, most of the early Eocene sedimentary record appears continuous with an average compacted sedimentation rate of 15 m/Myr (Shipboard Scientific Party, 2004). D'Onofrio et al. (2020) documented the plankic foraminiferal abundances across the interval of interest. A detailed bulk carbonate $\delta^{13}C$ record has been generated across part of the early Eocene at Site 1258 (Kirtland-Turner et al., 2014).

Site 1263 is located at 28°3′ S, 2°47′ E, and 2717 m water depth, a few hundred meters below the crest of Walvis Ridge (Zachos et al., 2004). During the early Eocene, the position was ~10° further to the south (Van Hinsbergen et al., 2015) with a water depth of ~1500 m (Zachos et al., 2004). Early Eocene sediments exhibit decimeter- to meter-scale bedding cycles, as expressed in magnetic susceptibility, colour reflectance and other physical property records (Zachos et al., 2004; Lauretano et al., 2015, 2016). These cycles are related to eccentricity and precession cycles and, because multiple holes were drilled at Site 1263, can be used to make a spliced sediment record with depths in rmcd (Westerhold et al., 2007, 2015). The site has good sedimentary recovery and an apparently complete lower Eocene succession that mainly consists of nannofossil ooze and nannofossil chalk. Considerable work has been conducted at Site 1263, including calcareous nannofossil and benthic foraminiferal information across the hyperthermals ETM2, H2, I1 and I2 (e.g., Dedert et al., 2012, 2014; Gibbs et al., 2012; D'Haenens et al., 2014) and data on planktic foraminiferal assemblages (Luciani et al., 2017b). In summary, there is a very solid stratigraphic framework for the early Eocene at Site 1263. The interval studied here is from 297 rmcd and 241 rmcd at Hole 1263B (the same as investigated by Luciani et al., 2017b).

The major changes in morozovellid coiling direction at the three sites investigated can be compared to variations in the bulk sediment $\delta^{13}C$ and $\delta^{18}O$ record. The negative CIEs exhibited across lower Eocene sediments correlate with widely recognized similar excursions at other locations on the basis of their bio-magnetostratigraphic position. These CIEs represent perturbations in the global carbon cycle and have been labelled at the sites studied according to an alphabetic scheme proposed by Cramer et al. (2003) and extended in subsequent works (e.g., Coccioni et al., 2012; Lauretano et al., 2016; Westerhold et al., 2018).

4. Paleoecology and geographical distribution of Eocene *Morozovella*

In order to better comprehend possible mechanisms for changes in coiling directions within morozovellids across the EECO interval, we briefly summarize the knowledge on their ecology and geographic distribution. During the early Eocene, morozovellids were widely distributed in (sub)tropical regions of all oceans, with the highest abundances at low latitudes. D'Onofrio et al. (2020) showed relative abundances of morozovellid species for the three locations described above (i.e., Sites 1258, 1051 and 1263). Morozovellids are significantly more abundant at Sites 1051 and 1258 compared to Site 1263, which is consistent with latitude and that morozovellids seemingly thrive in warm surface waters (Boersma et al., 1987; Pearson et al., 1993, 2001). This observation translates to different *Morozovella* species distributions. Prior to the EECO, *M. marginodentata, M. gracilis, M. subbotinae, M. aragonensis, M. crater* are more abundant at sites 1051 and 1258, indicating that their biogeographic optimum was at low latitudes. Furthermore, the zonal marker *M. aragonensis* first appears at the equatorial Site 1258 with the documented diachronism for the basal datum perhaps related to a warm-water preference for this species (Luciani et al., 2017a; D'Onofrio et al., 2020). Conversely, *Morozovella aequa* has a higher relative abundance at Site 1263, probably because this species preferred cooler temperatures at more temperate latitudes.

Stable isotope paleobiology is available for most of the Eocene planktic foraminiferal species (e.g., Pearson et al., 2006 and reference therein; Luciani et al., 2017a). Oxygen and Carbon isotopes values of morozovellids are compatible with a surface mixed-layer habitat similar to that inferred for *Acarinina*. Moreover, species of both genera display a pronounced increase in $\delta^{13}C$ with increased test size (above references). This strongly suggests algal photosymbiont activity because symbionts preferentially remove the lighter ^{12}C isotope and because larger specimens support greater dinoflagellate symbiont density (e.g., Spero and DeNiro, 1987).

A loss of photosymbionts (bleaching) should cause a reduction in test-size (e.g., Be et al., 1982). A bleaching episode may have occurred at

the beginning of the EECO at Site 1051 as test-size became smaller at this time for the species *M. formosa, M. gracilis, M. lensiformis*, and *M. marginodentata*Luciani et al. (2017a). Surprisingly, though, a restricted test-size continued through the EECO, even after stable isotope measurements suggest that algal photosymbiosis was restored (Luciani et al., 2017a). D'Onofrio et al. (2020) record at Site 1258, a test-size reduction when comparing the intervals below and above the J CIE. In particular, this reduction in maximum test size involves principally the species *Morozovella gracilis, M. marginodentata, M. subbotinae, M. formosa* and *M. crater*. The test size reduction does not involve the species *M. aragonensis* at Site 1258 that ranges up to the middle Eocene (e.g., Wade et al., 2011).

Test size-reduction in morozovellids during the EECO has been interpreted as a strategy to face environmental changes induced by the EECO perturbation (Luciani et al., 2017a; D'Onofrio et al., 2020). A possible explanation derives from the general decrease in $\delta^{13}C$ values between the mixed-layer dwellers and the thermocline dweller *Subbotina* spp. through the EECO. This could suggest that mixed-layer taxa became less reliant on photosymbionts because they moved to slightly deeper depths where light levels were lower (Luciani et al., 2017a). In any case, the size decrease in planktic foraminiferal tests probably implies the crossing of some ecological threshold.

Interestingly, many *Morozovella* species exhibit less extreme high $\delta^{13}C$ and low $\delta^{18}O$ values with respect to most acarininids, consistent with previous examinations of late Paleocene and Eocene foraminiferal assemblages (e.g., Shackleton et al., 1985; Boersma et al., 1987; Pearson et al., 2001; Quillévéré et al., 2001; John et al., 2013, 2014; Luciani et al., 2017a). Most morozovellids may have thus lived slightly deeper in the mixed-layer habitat with respect to acarininids or they may have sunk there at gametogenesis as suggested by the occurrence of a late stage gametogenic crust in the test and by the isotopic values. These features are especially evident in *M. aragonensis, M. lensiformis* (John et al., 2013, 2014) and to some extent in *M. aequa* and *M. subbotinae* (Luciani et al., 2017a). Nevertheless, the $\delta^{13}C$ record of single *Morozovella* species at Site 1051 (Luciani et al., 2017a) suggests that depth habitat changes were not significant and that various morozovellids retained a mixed-layer habitat, possibly a lower mixed-layer habitat, through the early Eocene. Prior to this study, there was no record on the possible differences in the ecology of the sinistral and dextral morphotypes of *Morozovella* within the mixed-layer.

5. Methods

To establish changes in morozovellid coiling direction, numerous discrete sediment samples were taken from lower to middle Eocene sections at the three aforementioned sites already studied for changes in morozovellid abundance. Fifty samples were selected from the Hole 1051A, between 452.3 mbsf and 353.1 mbsf. The sample spacing varied from 5 cm to 10 cm across the J event, from 40 cm to 200 cm within the EECO, and from 40 cm to 300 cm below and above the EECO, with time resolutions variable from 2 kyr to 30 kyr, on the basis of the orbitally-tuned age model at Site 1263 (Lauretano et al., 2016) extended at Site 1051 (Luciani et al., 2017b).

One hundred and forty eight samples were taken from Hole 1258A between 130.58 rmcd and 56.05 rmcd. The sample spacing varied from 10 cm to 100 cm with time resolution from 3 kyr to 20 kyr, according to the age model from Kirtland-Turner et al. (2014).

Sixty-eight samples were selected from Hole 1263B, spanning between 297.2 rmcd and 240.5 rmcd. The sample spacing varied from 20 cm to 100 cm with time resolution from 20 kyr to 170 kyr, on the basis of the age model proposed by Lauretano et al. (2016).

Relative abundances of planktic foraminiferal genera and morozovellid species have been published for all the three sites (Luciani et al. 2017a, b; D'Onofrio et al., 2020). Here we report in Figs. 3-5 the abundance of the genus *Morozovella* and of the morozovellid species for a direct comparison with the coiling changes.

Planktic foraminifera were extracted as follows. Sediment samples were disaggregated in deionized water over a time varying from a few hours to 3 days. Once disaggregated, samples were washed over a >63 μm sieve. Sieves were immersed in a methylene blue bath after each washing in order to colour planktic foraminifera potentially trapped in the sieve mesh (e.g., Green, 2001). This is an easy method to exclude possible contamination among successive samples. Washed residues were then dried at <50 °C, and examined under an incident light stereomicroscope for the morozovellid coiling direction in the >63 μm size-fraction from random splits using a Micro Riffle Splitter Gilson SP-171X.

Planktic foraminifera in all samples investigated exhibit "frosty" preservation (sensu Sexton et al., 2006). This implies some degree of calcium carbonate ($CaCO_3$) recrystallization, where some fraction of original test material formed in the mixed-layer has dissolved, and some fraction of present test material has precipitated at or beneath the seafloor. In some cases, tests are also infilled with $CaCO_3$, presumably added from pore water. In order to generate reproducible stable isotope records, specimens were picked after carefully checking for preservation, and removing tests with heavy recrystallization or obvious infilling. Such foraminifera tests should skew stable isotope signals, especially for oxygen (e.g., Pearson et al., 2001; Sexton et al., 2006; Edgar et al., 2013; Slotnick et al., 2015).

The taxonomic criteria for *Morozovella* species in this study follow those presented by Olsson et al. (1999) and Pearson et al. (2006). The taxonomic list of species cited in our text and figures is shown in Appendix A. Evaluation on changes in coiling direction was determined on the >63 μm fraction by counting the right-coiled (dextral) and the left-coiled (sinistral) specimens of *Morozovella*, within a population of ~180 specimens depending on availability. For the three sites investigated coiling direction was determined at the genus and species level. The counts are expressed in percentages (Figs. 3-5; Supplementary Tables S1-S3).

Considering that our quantitative analysis revealed changes in morozovellid coiling, we performed stable isotope analysis on DX and SN morphotypes from the >250 μm fraction on samples below the main coiling shift, at the initial phases of the coiling shift and in the interval post the coiling shift. These samples came from all three sites, and their stratigraphic positions are shown in Figs. 3-5. The number of species selected per interval was constrained by the availability of DX and SN morphotypes (Fig. 6). We picked ~40 specimens of DX and SN morphotypes of diverse species depending on availability. When individual morphospecies were restricted in abundance, approximately 40 specimens of SN and DX morozovellids belonging to diverse morphospecies were picked in equal proportion, referred to as *Morozovella* spp. Due to the scarcity of SN forms below and of DX specimens above the coiling shif, the *Morozovella* spp. stable isotope data refer to the three intervals only at Site 1051 whereas at sites 1263 and 1258 the analysis was only possible for the interval corresponding to the initial shift (Fig. 6). Data are shown in Fig. 6 and Supplementary Table 4.

Stable isotope analyses were performed at the Stable Isotope Laboratory of the Department of Geosciences at the University of Padova using a Thermo Scientific Delta V Advantage Isotope Ratio Mass Spectrometer coupled with a Gas Bench II automated preparation device. Samples of ~200–250 μg were crushed and flushed with helium and then treated with 10 mL of 100% phosphoric acid (EMSURE ® $\geq$ 99%) at 70 °C for ca 3 h. Isotopic values are reported in standard delta notation relative to the Vienna Pee Dee Belemnite (VPDB). During the analytical runs, an internal standard (white Carrara marble Maq 1: $\delta13C = 2.58‰$; $\delta18O = -1.15‰$ VPDB) was used to normalize raw $\delta^{13}C$ and $\delta^{18}O$ values and check standard (marble Gr1:; $\delta^{13}C = 0.68‰$; $\delta^{18}O = -10.44‰$ VPDB) was used to assess precision. Repeated analyses gave a precision better than 0.07‰ for $\delta^{13}C$, and better than 0.09‰ for $\delta^{18}O$.

6. Results

Morozovellid populations within early Eocene sediment at Sites

1051, 1258 and 1263 contain DX and SN forms (Figs. 3-5). The two different morphotypes are readily identified (Fig. 2). Most samples have populations with a strong preference (> 70%) for either DX or SN coiling. More interestingly, such coiling preference exists in multiple species and varies with sediment age. Our main result is the record of a change from preferentially dextral coiling to preferentially sinistral coiling soon after the start of EECO. Considering that the coiling switch closely followed the prominent drop in morozovellid abundance at all sites, the late dominance of SN motphotypes can be read as a fairly rapid and dramatic decrease in DX forms.

6.1. *Morozovella coiling-direction changes across the EECO at Site 1051*

The *Morozovella* population at Site 1051 moves from dominantly DX (91%) to dominantly SN (70%) tests across the studied interval (Fig. 3). Much of the change in coiling direction for the overall population spans 5.5 mbsf between 417.8 mbsf and 412.3 mbsf. The lower depth is ~10 m above the J event and the change in abundance; the upper depth lies ~3.5 m above the K/X event. The termination of the DX to SN coiling switch thus occurs close to the base of foraminiferal Zone E6/E7a.

An intriguing observation manifests in sediment below morozovellid coiling shift: transient excursions to higher abundances of sinistral tests occurred in conjunction with CIEs before and after the onset of EECO. Specifically, there are increases in sinistrally-coiled morozovellids that correlate with the ETM2, I-1 and J events (23%, 10% and 11%, respectfully) (Fig. 3). A sharp peak of sinistrally-coiled taxa (81%) also appears slightly above the J event (423.4 m).

Remarkably, the major shift in morozovellid coiling direction cuts across several species (*Morozovella aequa, M. gracilis, M. marginodentata, M. subbotinae*) (Fig. 3). In the upper part of C23r, above the major switch in coiling, only *M. crater* and *M. lensiformis* returned to near proportionally coiled morphotypes. All other species retained a dominant SN coiling. Most notably, populations of *M. aragonensis*, *M. caucasica* and *M. crater* are almost entirely sinistrally coiled (98%, 100%, 88% respectively) in lower middle Eocene sediments.

Transient increases in SN morphotypes abundance across pre-EECO CIEs also happened across most *Morozovella* species existing at this time (Fig. 3). For example, during the ETM2 event, SN morphotypes of *M. gracilis* and *M. marginodentata* reached peaks of 61% and 53%, whereas *M. crater* and *M. subbotinae* exhibited minor increases (18% and 23% respectively). Coincident with the I-1 event, SN morphotypes of *M. aequa* and *M. crater* rose to 46% and 17%, respectively. The SN morphotypes of *M. aragonensis* and *M. lensiformis* increase up to 50% (sample 428.19 mbsf) and 100% (sample 428.15 mbsf) respectively, close to the J event (~53 Ma), and those of *M. crater*, *M. gracilis* and *M. marginodentata* each peaks of 17%, 20%, 33%, respectively, about one meter above (~20 kyr after the J event) (Fig. 3).

6.2. *Morozovella coiling-direction changes across the EECO at Site 1258*

Like our observations at Site 1051, the *Morozovella* population in Eocene sediment at Site 1258 moves from dominantly DX (~93%) to dominantly SN (~85%) tests across the studied interval (Fig. 4). Much of this change in coiling direction again occurs over a relatively short depth interval, ~12 rmcd above the J event and ~ 4 rmcd above the K/X event, which are centered at 106.47 rmcd and 95.43 rmcd respectively.

At Site 1258 the *Morozovella* population moves from dominantly DX (~93%) to dominantly SN (~85%) tests across the studied interval (Fig. 4). Much of the change in the coiling direction for the overall population occurs ~4 m above the K/X event, at 95.43 rmcd. This change occurred ~12 rmcd above the drop in morozovellid abundance that is recorded at Site 1258 ~ 20kyr before the J event. Transient excursions to increased abundances of SN tests before the major coiling shift also happened during brief CIEs at Site 1051 (Fig. 4). A small peak in SN *Morozovella* at the ETM2 event (20%) corresponds in magnitude to that observed at Site 1051 (23%). At Site 1258, however, an increase in

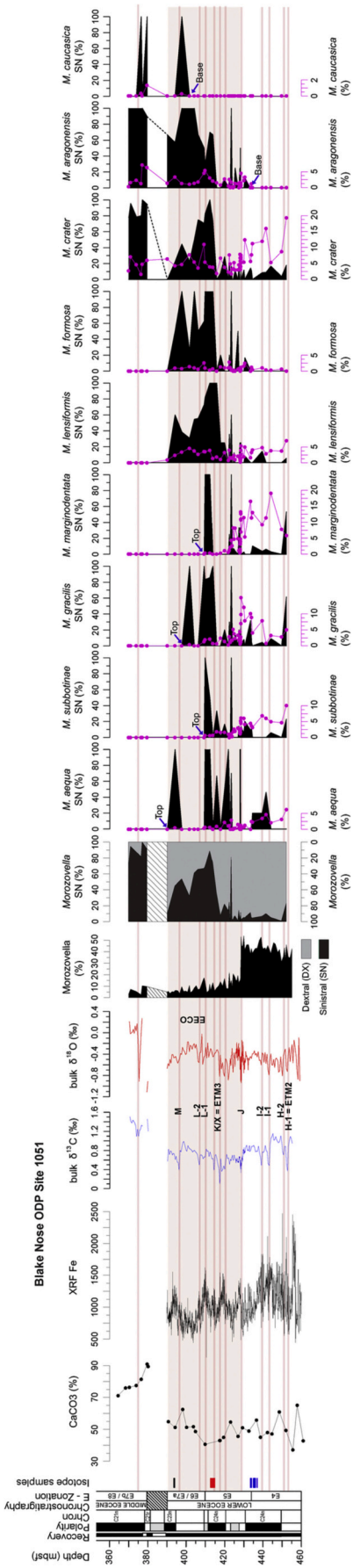

Fig. 3. Changes in coiling direction within the *Morozovella* genus (≥63 μm size fraction) at Site 1051. Bulk $\delta^{13}C$ and $\delta^{18}O$ records are from Luciani et al. (2017a). The main carbon isotope excursions are labelled according to Westerhold et al. (2018). The $CaCO_3$ record is from Norris et al. (1998) The XRF Fe count record is from Röhl et al. (2003). The relative *Morozovella* abundance and of each *Morozovella* species abundance is also shown (pink curves) (data from Luciani et al., 2017a). Note the marked but transitory flip from dominant dextral to dominant sinistral coiling of the *Morozovella* genus slightly above the J event and the remarkable change from dominant DX to dominant SN coiling above the K/X event. Moderate increases of sinistral morphotypes occurred during some pre-EECO CIEs, which are known or presumed hyperthermals. Both the long-lasting and transitory flips from dominantly DX to dominantly SN coiling involved all the *Morozovella* species. The position of samples selected for the stable isotope analyses on DX and SN morphotypes are indicated by the blue (interval below the coiling shift), red (initial coiling shift interval) and black (post-coiling shift interval). (For interpretation of the references to colour in this figure legend, the reader is referred to the web version of this article.)

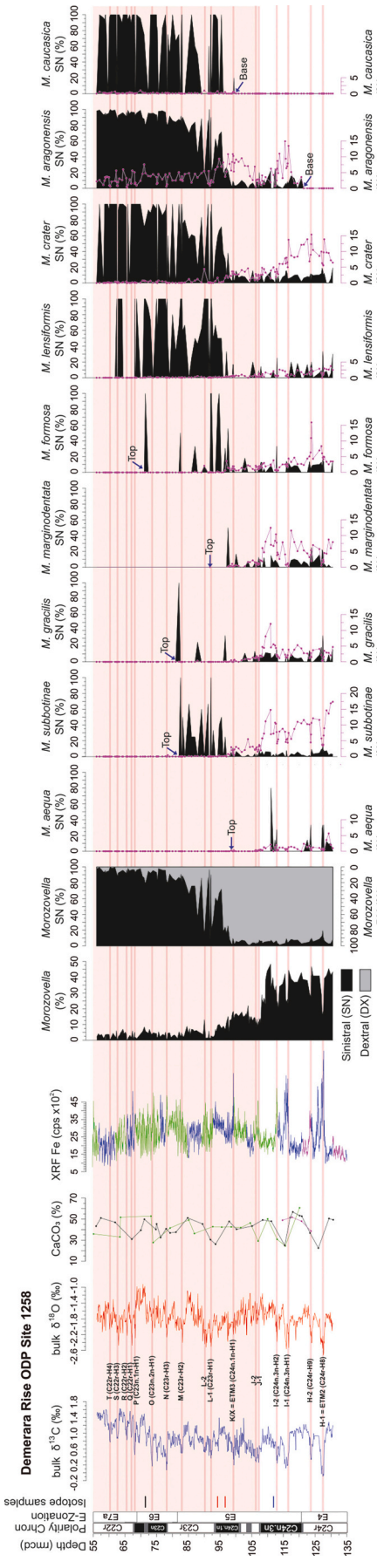

Fig. 4. Changes in coiling direction within *Morozovella* genus and species (≥63 μm size fraction) across the EECO at the ODP Site 1258. Bulk isotope records ($\delta^{13}C$, $\delta^{18}O$) are from Kirtland-Turner et al., 2014). The main carbon isotope excursions are labelled according to Westerhold et al. (2018). The carbonate content ($CaCO_3$ curve) is from Sexton et al. (2011). The XRF (X-Ray Fluorescence) Fe content is from Westerhold et al. (2017) (green curve from Hole 1258A, blue curve from Hole 1258B, pink curve from Hole 1258C). The relative abundance of *Morozovella* genus and of the single species of *Morozovella* is also shown (pink curves) (data from D'Onofrio et al., 2020). Note that, also at Site 1258 a switch to dominant SN coiling occurred above the K/X event. The dominant DX coiling prevailed in all morozovellids below the EECO interval. Moderate increases of SN morphotypes occurred during some pre-EECO CIEs, similarly to what observed at Site 1051. The position of samples selected for the stable isotope analyses on DX and SN morphotypes are indicated by the blue (interval below the coiling shift), red (initial coiling shift interval) and black (post-coiling shift interval). (For interpretation of the references to colour in this figure legend, the reader is referred to the web version of this article.)

SN coiling morozovellids correlates with the H2 event (10%), and only some species show minor SN coiling peaks with the I2 event (27% of *M. aequa*; 15% of *M. gracilis*; 34% of *M. formosa*; 25% of *M. lensiformis*). Moreover, several short peaks of SN coiling occurred in the interval of dominant DX coiling which do not correlate with CIEs. For example, maxima appear in records of *M. aequa* (80% SN) slightly above the I2 CIE, and in *M. gracilis* (33% SN), *M. formosa* (56% SN) and *M. marginodentata* (50% SN) slightly above the K/X CIE, although these do not coincide precisely.

The major shift in morozovellid coiling direction involves at Site 1258 all species, both those species that disappear within the EECO (*Morozovella aequa, M. formosa, M. gracilis, M. lensiformis, M. marginodentata, M. subbotinae*; Fig. 4) and those species that have a longer stratigraphic range *(M. lensiformis, M. aragonensis, M. caucasica, M. crater*).

6.3. *Morozovella coiling-direction changes across the EECO at Site 1263*

The *Morozovella* genus displays trends in coiling direction at Site 1263 similar to those recorded at sites 1051 and 1258 (Figs. 5). Again, a remarkable and persistent switch from dominantly DX (~68%, mean value) to dominantly SN (~80%, mean value) forms happened between the J event and slightly above the K/X event and involves all the species of *Morozovella*. We have not precisely documented the change because of a 2.5 m gap between cores 23H and 22H in Hole 1263B. However, future work using sediment from other holes at this site should improve the detail. The coiling change occurred ~3 to 5.5 rmcd above the drop in morozovellid abundance that is recorded ~165 kyr after the J event (Luciani et al., 2017b).

The species that display a greater average number of sinistrally coiled morphotypes below the major coiling shift are *M. aequa* and *M. lensiformis*. The species *M. marginodentata, M. gracilis, M. crater* and *M. aragonensis* display, instead, transient peaks in SN coiled morphotypes. However, the intervals of increased sinistrally coiled tests are different to the record observed at sites 1051 and 1258, as they do not correspond at Site 1263 to CIEs (Fig. 5). An exception is represented by the ETM2 that records a temporary shift to SN morphotypes of *M. aequa, M. crater* and *M. lensiformis* of up to ~80% each. Sinistrally coiled *M. aequa* (94%) and *M. lensiformis* (80%) are also recorded coinciding with the H2 event.

6.4. *Stable isotope data on SN and DX morozovellid morphotypes*

To evaluate possible differences in habitat or shifts within the water column of the diverse morphotypes, we performed carbon and oxygen stable isotope analyses on a number of dextrally and sinistrally coiled specimens of *Morozovella* from levels below, at the initial and above the major coiling shift at all three sites. Significantly, our results revealed that SN and DX morozovellids belonging to the same morphospecies show different stable isotope values (Fig. 6).

Considering that foraminifera at the three sites studied do not show a 'glassy' preservation (sensu Sexton et al., 2006), the degree of recrystallization implied by the observed 'frosty' preservation may have influenced the oxygen stable isotope data and thus cannot be used to achieve reliable paleotemperatures. However, differences in the mean $\delta^{18}O$ values were recorded at the three sites. Specifically, the most negative $\delta^{18}O$ values occur at the equatorial Site 1258. The $\delta^{13}C$ values are less influenced by recrystallization (e.g., Frank et al., 1999; Edgar et al., 2013, 2015) and may be interpreted as revealing the position that the morozovellids occupied within the mixed-layer and photosymbiotic associations.

Our data from Site 1263 show than DX morphotypes belonging to *M. aequa* and *M. subbotinae* record more positve $\delta^{13}C$ with respect to sinistrally coiled *M. aequa* and *M. subbotinae* ($\Delta = 0.47‰$ and $\Delta = 0.28‰$ respectively) (Fig. 6 A) in the interval preceding the coiling shift. Similarly, in the interval of the initial coiling shift, the analysis on

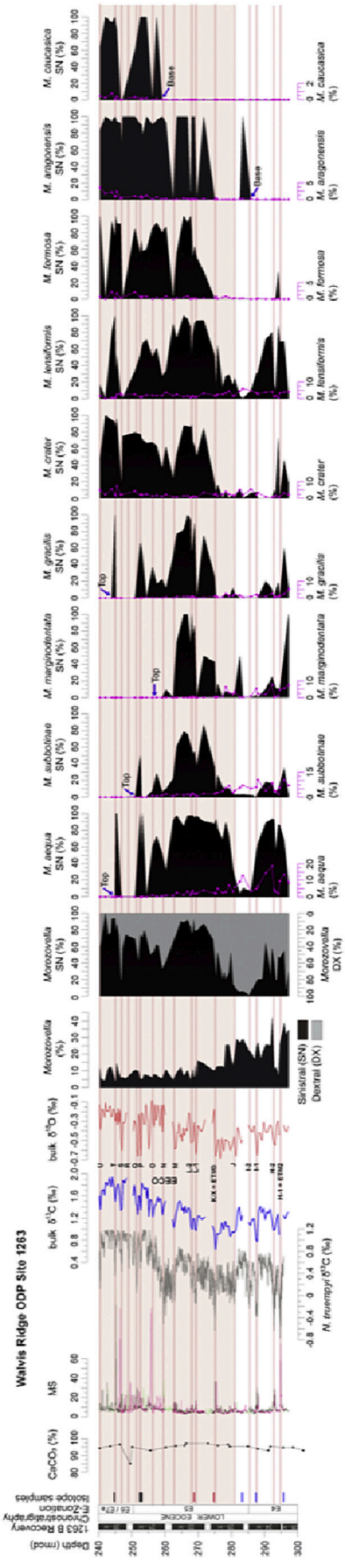

Fig. 5. Changes in coiling direction within *Morozovella* genus and species (≥63 μm size fraction) across the EECO interval at Site 1263. The $\delta^{13}C$ record from benthic foraminifera (*N. truempyi*) comes from Lauretano et al. (2016) (grey) and the bulk sediment $\delta^{13}C$ record is from Luciani et al. (2017b.) The main carbon isotope excursions are labelled according to Westerhold et al. (2018). The carbonate content ($CaCO_3$) and MS (magnetic susceptibility) records are from the Shipboard Scientific Party (2004). The green, black and pink colours in the MS profile come from Holes 1263A, 1263B and 1263C, respectively. The relative abundance of *Morozovella* genus and of the single species of *Morozovella* is also shown (pink curves) (data from D'Onofrio et al., 2020). DX coiling morozovellids prevailed below the EECO interval and a switch to dominant sinistrally coiled mode is recorded after the K/X event, as observed at sites 1051 and 1258. At Site 1263 the increases of SN morphotypes during pre-EECO CIEs has not been observed. The position of samples selected for the stable isotope analyses on DX and SN morphotypes are indicated by the blue (interval below the coiling shift), red (initial coiling shift interval) and black (post-coiling shift interval). (For interpretation of the references to colour in this figure legend, the reader is referred to the web version of this article.)

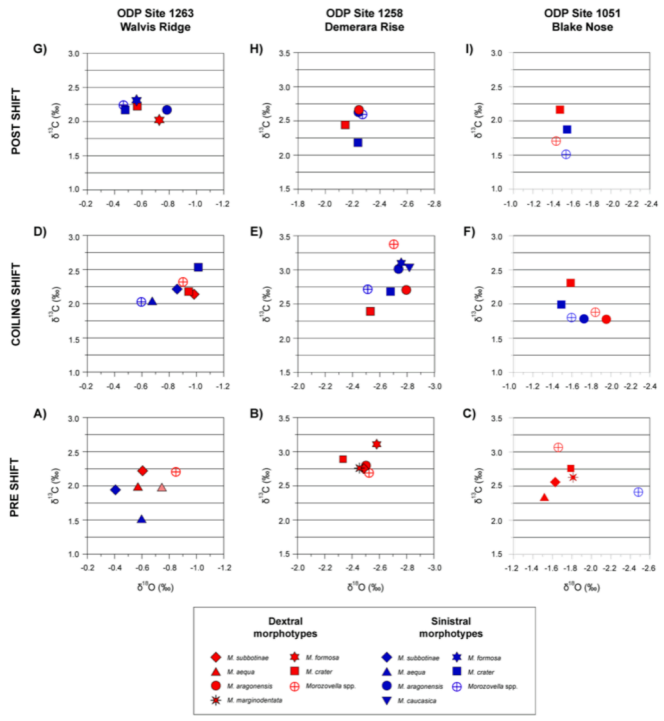

Fig. 6. Stable carbon and oxygen data from DX (red symbols) and SN (blue symbols) morphotypes of selected *Morozovella* species from three intervals: (A, B, C) pre-coiling shift, (D, E, F) initial coiling shift, (G, H, I) post coiling shift at the Atlantic sites 1263, 1258 and 1051. The position of samples examined is shown on Figs. 3-5. The selection of morphospecies is necessarily restricted to the forms with enough DX and SN morphotypes for the isotope analysis. *Morozovella* spp. include all morozovellids occurring in the examined samples in nearly equal proportion of each morphospecies. Note that in most cases the SN morphotypes record lower $\delta^{13}C$ values. This may imply that the SN forms were less dependent on their photosymbiotic partnerships and thus able to adapt more readily to paleoceanographic change within the EECO. (For interpretation of the references to colour in this figure legend, the reader is referred to the web version of this article.)

Morozovella spp. reveals that DX forms record higher $\delta^{13}C$ values than SN tests ($\Delta = 0.29‰$) (Fig. 6 D). However, the species *M. crater* displays an 'inverse' record because the DX morphotypes have lower $\delta^{13}C$ values (2.18‰) with respect to the SN tests (2.54‰) ($\Delta = 0.36‰$), as well as *M. subbotinae* DX with respect to the SN morphotypes ($\Delta = 0.8‰$) (Fig. 6 D). In the post-coiling shift interval *M. crater* SN records lower $\delta^{13}C$ values than DX ($\Delta = 0.6‰$). Conversely, *M. formosa* SN has higher $\delta^{13}C$ values than DX morphotypes ($\Delta = 0.29‰$) (Fig. 6 G).

At Site 1258 due to the scarcity of SN morphotypes from the pre-coiling shift interval no data are available for these forms (Fig. 6 B). At the initial coiling-shift interval, both *M. aragonensis* SN and *M. crater* SN had higher $\delta^{13}C$ values than related DX morphotypes ($\Delta = 0.31‰$ and $\Delta = 0.29‰$ respectively). Opposite $\delta^{13}C$ values were obtained for the *Morozovella* spp. In fact, the SN morphotypes give distinctly lower values that DX tests ($\Delta = 0.66‰$) (Fig. 6 E). In the post-coiling shift interval, the $\delta^{13}C$ value returns to lower values for SN tests of *M. crater* with respect to the DX morphotypes ($\Delta = 0.27‰$) whereas *M. aragonensis* DX and SN show very close $\delta^{13}C$ values (2.66‰ and 2.63‰ respectively) (Fig. 6 H).

In the pre-coiling shift interval at Site 1051 we were able to obtain $\delta^{13}C$ values for both SN and DX *Morozovella* spp. morphotypes. Results show that the former were isotopically lighter than the latter ($\Delta = 0.66‰$) (Fig. 6 C). The initial coiling-shift interval records the same result for the *Morozovella* spp. SN and DX, though with minor differences in the values ($\Delta = 0.08‰$). In this interval, also *M. crater* SN gives lower values that DX morphotypes ($\Delta = 0.33‰$) whereas SN and DX tests of

M. aragonensis display the same values ($\delta^{13}C = 1.78‰$) (Fig. 6 F). Data on the post-shift interval are refereed to *M. crater* SN and DX and on *Morozovella* spp. SN and DX that reveal lower values for all SN morphotypes ($\Delta = 0.29‰$ and $\Delta = 0.19‰$, respectively) (Fig. 6 I).

7. Discussion

7.1. Early Eocene coiling changes in Morozovella and carbon cycle perturbations

Modifications in *Morozovella* coiling direction are associated with CIEs and established changes in the global carbon cycle and temperature. As expressed by the records at sites 1051, 1258 and 1263 (Figs. 3-5), the relationship between the coiling character of morozovellids and carbon cycle perturbations during the early Eocene is complex.

The five main findings are: (1) a permanent switch from dominantly DX to dominantly SN coiling occurred at the start of the EECO at three widely separated locations; (2) the major switch in coiling direction follows the permanent drop in morozovellid abundance; (3) transient changes in coiling direction happened at sites 1051 and 1258 before the major coiling switch, in several cases during negative CIEs before the EECO; (4) the changes in coiling direction spanned multiple species; (5) SN morphotypes typically have lower $\delta^{13}C$ values.

Two basic observations underscore potential complexities between changes in *Morozovella* abundance and coiling direction. First, for the totality of morozovellids, the decline in abundance precedes the shift in coiling (Figs. 3-5). At the three sites investigated, the adundance drop began close to the J event (Luciani et al., 2016, 2017a, b; D'Onofrio et al., 2020) whereas the coiling change happened <200 Kyr after the K/X event. On the basis of the orbitally-tuned age model at Site 1263 (Lauretano et al., 2016) and of the astronomical calibration at several sites, including Site 1263 (Westerhold et al., 2017, 2018), approximately 400 Kyr transpired between the J and K/X events. Thus, within about the first ~600 Kyr of the EECO, the abundance and coiling direction of morozovellids changed markedly. Notably, the changes in abundances and coiling direction spanned multiple morphologically defined species (Figs. 3-5). Our data on the timing of the abundance crash and coiling shift represent additional biostratigraphic events that can be utilized as markers in marine sections elsewhere.

A major change in the overall morozovellid assemblage occurred across the J event, with a loss of DX morozovellid tests (Figs. 3-5). This is clearly shown at Site 1051 by plotting the abundance of DX morphotypes relative to the total number of planktic foraminifera in the samples (Fig. 7). The coiling shift can thus be (partly) explained through the decrease predominately in the abundances of DX morphotypes of morozovellid species (or DX cryptic species).

Interestingly, some of the temporary changes towards preferred SN coiling occurred in morozovellid populations at sites 1051 and 1258 during at least some of the geologically brief early Eocene hyperthermals (e.g., ETM2, H2, I1), which seemingly shared some environmental characteristics (e.g., warming) with the much longer EECO. At the ETM2, which represents one of the major hyperthermals, a more consistent transitory shift to SN morphotypes occurred that reached 20–23% at sites 1051 and 1258 and up to ~80% of SN *M. aequa, M. crater* and *M. lensiformis* at Site 1263. That stated, it is probably not a coincidence that the overall changes in abundance and coiling direction of multiple morozovellid species observed for the prolonged initial phase of EECO also happened to a lesser degree over shorter hyperthermal events. Seemingly, for some reason, the characteristic trait(s) for DX coiling in morozovellids was not favourable during times of mixed-layer warming and/or related hyperthermal geochemical changes.

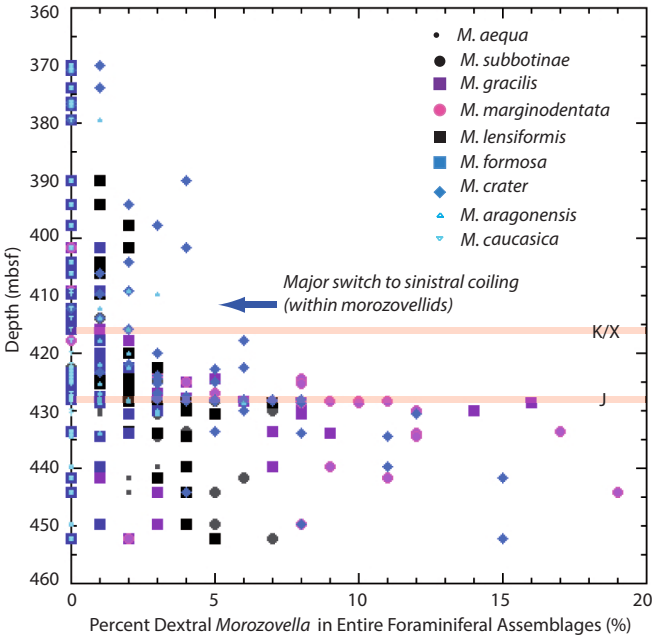

Fig. 7. The abundance of DX morphotypes of *Morozovella* species at Site 1051 plotted in terms of abundance of the total planktic foraminiferal assemblage. Here it becomes clear that the basic cause of the major coiling switch is a loss of DX specimens, whether they were different morphotypes of species or cryptic species, occurring at the J event.

7.2. Coiling changes within the different Morozovella species at sites 1051, 1258 and 1263

In regards to the coiling change within different *Morozovella* species at the sites investigated we can attain some interesting reflections. Despite differences in relative abundance of the different species across the sites, as expected from the diverse latitude represented, all the species at all sites modify their coiling within the EECO from preferentially DX to SN after the K/X event. In particular, at Site 1258 we record the highest percentage of SN morphotypes for each morphospecies that is near the 100% for *M. lensiformis, M. crater*, *M. aragonensis* and *M. caucasica.* At Site 1051, *M. lensiformis, M. crater* and *M. aragonensis*, after a prominent and protracted dominance of SN mode following the K/X event, had an almost equivalent occurrence of DX and SN forms for its remaining early Eocene existence. The species *Morozovella crater* followed similarly, but did not go extinct during the EECO and became almost exclusively SN in the early middle Eocene. *Morozovella aragonensis* preserved its newly found SN coiling mode throughout the EECO and beyond. Similar behaviour is shown by *M. lensiformis M. crater* and *M. aragonensis* at Site 1263.

Interestingly, Pearson (1993) noted, in agreement to Bolli (1950) and Luterbacher (1964), that at multiple low latitude locations *M. lensiformis*, *M. caucasica* and *M. aragonensis* reversed their preferred direction of coiling from DX to SN at the extinction level of the *M. subbotinae*. These observations also may agree with our records, even though the extinction level of *M. subbotinae* has revealed to be diachronous, as noted by Luciani et al. (2016), Luciani et al. (2017b) and D'Onofrio et al. (2020). Therefore, a correct correlation is not possible because the aforementioned earlier works were not calibrated with stable isotope stratigraphy nor related to changes in foraminiferal abundance.

Our data indicate that early Eocene morozovellids show different coiling direction through the interval investigated, even after maintenance of a preferred coiling direction for a prolonged time interval. This interpretation partly conflicts with ideas presented by Norris and Nishi (2001), who suggested that Paleogene planktic foraminifera preserve,

within each species, a preferential coiling direction from radiation until extinction. Moreover, the consideration that species with proportionate coiling are less susceptible to extinction because they are more genetically flexible and that they are more prone to generate new clades with respect to species with preferential coiling (Norris and Nishi, 2001) does not accord with our data. For example, *M. lensiformis* disappeared shortly after changing to proportionate coiling (Figs. 3, 5) and did not generate new clades. On the contrary, *M. aragonensis*, which gained almost exclusive SN coiling after the start of the EECO and therefore should be more susceptible to extinction, was the most long-lived morozovellid species (from base of Zone E5, ~ 52.3 Ma, to top of Zone E9, ~ 43.6 Ma; e.g., Toumarkine and Luterbacher, 1985; Norris and Nishi, 2001; Pearson et al., 2006; Aze et al., 2011; Wade et al., 2011). Our record therefore proves both that return to a rather proportionate coiling mode within morozovellid population is more frequent than previously thought, and this does not ensure longevity for the species nor the appearance of new clades. Further evidence that morozovellids were able to move from one coiling direction to another over relatively short interval of time, are the flips to SN coiling shown by the morozovellids before the EECO (Figs. 3-5). Whether SN and DX morphotypes were in fact cryptic species, environmental conditions temporarily (below the EECO) and permanently (after the K/X CIE) favoured SN cryptic species. However, other controlling factors, both environmentally or genetically driven, may have induced the temporary shifts to SN morphotypes that do not correspond to CIEs. In general, according to our data, changes in coiling direction do not relate to extinctions at the investigated Atlantic sites, unless SN and DX morphotypes were cryptic species, and then we see the almost total demise of DX morozvellid species.

7.3. Morozovellid coiling and reproductive mode

It is well known that benthic foraminifera can adopt alternatively sexual or asexual reproductive modes resulting in dimorphic shells that show differences in size and proloculus. Specifically, smaller shells with larger proluculi derive from asexual reproduction whereas larger shells bearing smaller proloculi originate by gametic reproduction (e.g., Sen Gupta, 2002). On the contrary, planktic foraminifera are considered to adopt only gametic reproduction (e.g., Hemleben, 1989). However, possible asexual reproduction has been observed for *N. pachyderma* in laboratory cultures (Kimoto and Tsuchiya, 2006; Davis et al., 2020), and this feature was considered as a possible driving factor controlling *N. pachyderma* coiling mode (e.g., Kimoto and Tsuchiya, 2006; Khare et al., 2012). Thus, the possibility that asexual reproduction influenced the coiling direction in Eocene planktic foraminifera is discussed below.

At sites 1051 and 1258, we have observed a reduction in maximum test-size in most morozovellid species near the start of the EECO (Luciani et al., 2017a; D'Onofrio et al., 2020), and when coiling mode changed from dominantly DX to SN. This might give evidence that smaller forms could be derived from asexual reproduction even though the small size can be linked to many other factors. Nevertheless, the decrease in maximum test size occurred at Site 1051 for some species (*M. gracilis, M. marginodentata*) below the onset of the EECO (Luciani et al., 2017a) and where DX coiling dominated (Fig. 3). Therefore the hypothesis that early Eocene switches in coiling direction were controlled by asexual reproduction seems improbable, especially because it has not been effectively demonstrated for living planktic foraminifera.

7.4. Paleoecology of DX and SN Morozovella morphotypes: Insights from carbon isotope results

Carbon isotope data from DX and SN morphotypes from the three ODP sites analysed, record variations between the two forms. DX morphotypes have generally more positive $\delta^{13}C$ with respect to SN forms, although some differences exist among the three sites examined, among the diverse morphospecies and through time (Fig. 6 and Table S4). Specifically, during the pre-coiling shift, i.e., below the EECO interval when DX coiling is dominant, available data suggest than DX morphotypes record more positive carbon isotope values (Fig. 6 A, C). Interestingly, Feldmeijer et al. (2015) record more positive stable isotope values for dextral *Globorotalia truncatulinoides*, a taxon that includes five cryptic species. Specifically, Feldmeijer et al. (2015) demonstrate a deeper calcification depth for sinistral *G. truncatulinoides* compared to dextral *G. truncatulinoides* from Termination III at North Atlantic and employ this evidence together with the dominance of the two morphotypes to trace the thermocline variations.

At the initial coiling shift, after the K/X event, the DX morozovellids again have more positive $\delta^{13}C$ signatures than SN morphospecies at all the sites investigated (Fig. 6 D, E, F). However, at sites 1263 and 1258, *M. crater* SN, *M. subbotinae* SN and *M. aragonensis* show an inverse record producing heavier $\delta^{13}C$ values with respect to the DX forms (Fig. 6 D, E). Data from *Morozovella* spp. derive from the species *M. aequa, M. gracilis, M. marginodentata, M. lensiformis* and *M. formosa* for which it was not possible to obtain species-specific stable isotope analyses.

In the interval after the coiling shift when SN coiling is steadily dominant, *Morozovella* spp. SN and *M. crater* SN revealed lighter $\delta^{13}C$ signatures with respect to DX morphotypes at all sites examined (Fig. 6 G, H, I). The species *M. formosa* SN represents an exception because, at Site 1263, it shows a heavier $\delta^{13}C$ values with respect to the DX equivalent (Fig. 6 G).

The more separated stable isotope values between DX and SN forms are recorded at the equatorial and tropical sites. It is possible that the observed separated values occurred at the low-latitude sites where temperature and other geochemical-physical parameters were more differentiated throughout the upper water column.

The offset in $\delta^{13}C$ values between SN and DX forms highlights that each morphospecies had a different ecology, as already suggested by the abundance data. One possibility is that the SN calcified at deeper depths within the mixed-layer. However, $\delta^{18}O$ values are only partly consistent with this depth habitat hypothesis, perhaps due to partial test recrystallization that occurred at or beneath the seafloor. Alternatively, the lower $\delta^{13}C$ signal in SN morphotypes may reflect reduced symbiont acquisition and requirements. Both metabolism and symbiont arrangement influence the carbon isotope signature of Eocene planktic foraminifera (Gaskell and Hull, 2019). It has already been shown the relationship between photosymbionts and their morozovellids hosts is volatile with several instances of bleaching (Wade et al., 2008; Luciani et al., 2017a). The resulting dominance of SN morphotypes, at the expense of DX forms, coupled with the lower $\delta^{13}C$ signatures, suggests that the SN forms were less dependent on their photosymbiotic partnerships and thus able to adapt more readily to paleoceanographic change. Following this scenario, slightly deeper habitat of SN forms, as can be suggested by $\delta^{13}C$ data, would be compatible. The reduction in the maximum test sizes observed across the EECO at all sites investigated (Luciani et al., 2017a, 2017b; D'Onofrio et al., 2020) involves the dominant survived SN morphotypes and may further support reduced photosymbiotic activity because attainment of large test sizes in symbiotic species is an indication of ecological success as a consequence of symbiont nutrition and such size reduction could imply symbiosis became less important for sustenance. Causes for the observed ecological behaviour can be manifold. However, the link with potential stressors occurred during the EECO interval and the demise of DX morphotypes appears consistent. Stressors may include extreme temperatures, pH changes, ultraviolet-light excess, reduced nutrients. Further detailed investigation is needed to reconstruct a comprehensive scenario. We cannot exclude that modifications in potential algal-symbiont assemblages (dinoflagellates) might have had a role.

By considering DX and SN forms as belonging to the same species, i.e., ecophenotypical morphotypes, our results indicate that some species were able to change their habitat through time. Alternatively, SN and DX cryptic species proved to have had this ability. Within this scenario, the successful SN morphotypes or sinistrally coiled cryptic species within

the EECO may be explained with their reduced photosymbiont activity and/or lower position in the mixed-layer with respect to DX forms.

7.5. Change in coiling direction: genetically or environmentally driven?

Taking note of the evidence described above, it remains to be determined whether the observed variations in coiling direction are genetically or environmentally driven. Evidently, the fossil record does not allow us to definitively prove the genetic origin of the observed morphotypes and we can therefore just evaluate different scenarios.

Norris and Nishi (2001) interpreted the coiling patterns in Paleogene tropical planktic foraminifera as heritable through time and not resulting from environmental control. According to these authors, changes in coiling direction are possible because species retain a genetic key that allows them to coil one way or the other. We cannot validate or disprove a genetic origin for the observed morphotypes in morozovellids at the examined sites nor can we demonstrate that these morphotypes might have diverged genetically in different species through adaptation to diverse environmental conditions. Further, we cannot exclude that, within any species defined by morphology, the DX and SN forms were different morphotypes exclusively influenced by ecology rather than cryptic speciation. However, our data shed new light on the stable-isotope derived paleobiology of DX and SN forms. Our data suggest that reduced algal photosymbiont activity favoured SN morphotypes. It is thus possible that only morphotypes sinistrally coiled had enough flexibility to keep the optimal environmental conditions for their survivorship across the EECO. One probable explanation is that observed SN and DX coiling of morozovellids were genetically heritable characteristics and that these lie within cryptic speciation across multiple morphologically defined species. From studies of recent planktic foraminifera, cryptic speciation is probably induced by a clear separation within water masses with different chemical and physical parameters through para-patric speciation, thus environmental and genetic control can be somewhat related (e.g., Ujiié et al., 2010; Ujiié and Asami, 2014; Morard et al., 2016). In the genetically controlled scenario, cryptic species with SN coiling demonstrate better adaptations to environmental conditions across the start of the EECO than cryptic species with DX coiling. The end-member alternative is that observed coiling changes were exclusively ecophenotypic responses whereby different species were able to preferentially adopt SN coiling to adapt to conditions that persisted in the mixed-layer conditions during the EECO. In Figs. 3-5 we show the carbonate, MS and XRF Fe content at the sites investigated to highlight whether changes in sedimentology coincide with the morozovellid coiling shift and whether these possible changes can give insight on environmental variations. A decrease in XRF Fe values is visible in Site 1051 from the I2 CIE, i.e., well below the morozovellid decline and coiling shift that occurred at the J event and above the K/X event respectively (Fig. 3). The observed $CaCO_3$ content and XRF Fe decreases is probably linked to the siliceous component increase (Luciani et al., 2017a) because the decline in abundance of morozovellids was likely balanced by the acarininid increase. No major changes in the carbonate content are present in sites 1258 and 1263 (Figs. 4,5). The magnetic susceptibility and XRF Fe generally increase at these sites in coincidence with the CIEs, as expected due to the carbonate dissolution. In conclusion, the carbonate content, magnetic susceptibility and XRF Fe data do not give evidence of major changes across the main coiling shift of morozovellids.

7.6. What caused the observed coiling change?

Several and potentially concomitant mechanisms may have caused the observed coiling change. Clearly, we need more effort to verify whether sea-surface variations (e.g., temperatures, pH, food availability, ultraviolet light excess) directly corresponded to the observed coiling variation. This effort includes a more comprehensive knowledge of the EECO. However, while the PETM has received considerable attention, records across the EECO remain scarce, so that we do not know the full suite and speed of environmental change. Recent records (Anagnostou et al., 2016) suggest high pCO_2 and possibly low surface-water pH. Inglis et al. (2020) estimated the global mean surface temperatures (GMST) from the EECO as ca 27 °C, that is 10 °C to 16 °C warmer that pre-industrial time. However, detailed paleotemperatures across the observed coiling changes are absent at present from the sites we analysed. The available $\delta^{18}O$ records from the three sites studied are affected by a certain degree of planktic foraminiferal recrystallization (Luciani et al., 2017a, 2017b; D'Onofrio et al., 2020) and calcareous nannofossil overgrowth at Site 1051 (Mita, 2001), so that calculated temperatures represent a combination of a primary surface water signal and a secondary diagenetic signal. We do note, though, that despite likely overprinting, major variations in temperature across the early to early middle Eocene appear evident in bulk carbonate $\delta^{18}O$. Specifically, a trend towards lighter values (i.e., warmth), at least at Site 1051, clearly manifests in the interval between the J and K/X events as well as during known and suspected hyperthermal events (Fig. 3). Other temperature proxies at Site 1051, such as TEX_{86} (Luciani et al., 2017a), indicate across the J event temperatures as high as ~32.6 °C (according to the Liu et al., 2009 calibration) or ~ 36.0 °C (according to the Kim et al., 2010 calibration). However, this analysis was restricted to one level at Site 1051 due to the scarcity of lipids (Luciani et al., 2017a) and is presently lacking for sites 1263 and 1258.

Changes towards increased surface water eutrophy have been invoked as a mechanism for coiling switches in planktic foraminifera (e.g., Khare et al., 2012 and reference therein), as, for example, supposed for the flip to SN preference of the late Paleocene *Igorina albeari* and for a DX coiling preference of *Rotalipora cushmani* during the latest Cenomanian (Hancock, 2005; Coccioni et al., 2016). Surface waters at Site 1051 may have experienced increased nutrient availability during the EECO, given the high biogenic silica flux (Witkowski et al., 2020b) and the abundance of radiolarians (Luciani et al., 2017a), which may reflect eutrophication (e.g., Hallock, 1987). Surface-water eutrophy at Site 1051 during the EECO seems also supported by the early Eocene calcareous nannofossil assemblages dominated by the eutrophic *Coccolithus pelagicus* (e.g, Tremolada and Bralower, 2004; Agnini et al., 2009). However, diatom assemblages have high percentages of hemiauloids (Witkowski et al., 2020b, 2021) indicating an oligotrophic conditions at Site 1051 during the EECO. Furthermore, on the basis of planktic foraminiferal assemblages and the absence of a siliceous component, no indication for increased surface water eutrophy exists at Site 1263 and 1258 (Luciani et al., 2017b; D'Onofrio et al., 2020), which clearly also have a switch to SN coiling within the *Morozovella* genus (Fig. 7). Therefore, we cannot attribute the observed switch to increased surface water eutrophy.

7.7. Coiling change as a biostratigrahic tool

Correlative changes between planktic foraminiferal coiling direction and the surface water environment have proven to be useful for stratigraphic correlation and paleoenvironmental interpretations in late Neogene sediments. This is true whether the morphotypes happen to be genetically distinct species or ecophenotypic types (e.g., Saito, 1976; Keigwin, 1978; Hooper and Weaver, 1987; Hodell et al., 1994, 2001; Berggren et al., 1995; Wade et al., 2011).

Our records from sites 1051, 1258 and 1263 suggest that morozovellid coiling variations, independent of causal mechanisms, have potential as a useful biostratigraphic tool for correlation. The three selected sites represent disparate settings in the Atlantic Ocean, a subtropical northern hemisphere, equatorial setting and temperate southern hemisphere latitude respectively (Ogg and Bardot, 2001; Van Hinsbergen et al., 2015). The prominent shift to SN coiling became permanent within ~200 Kyr after the K/X event (Fig. 8, Table 1).

Beyond understanding the cause of the coiling direction switches, such correspondence stimulates further high-resolution studies coupled

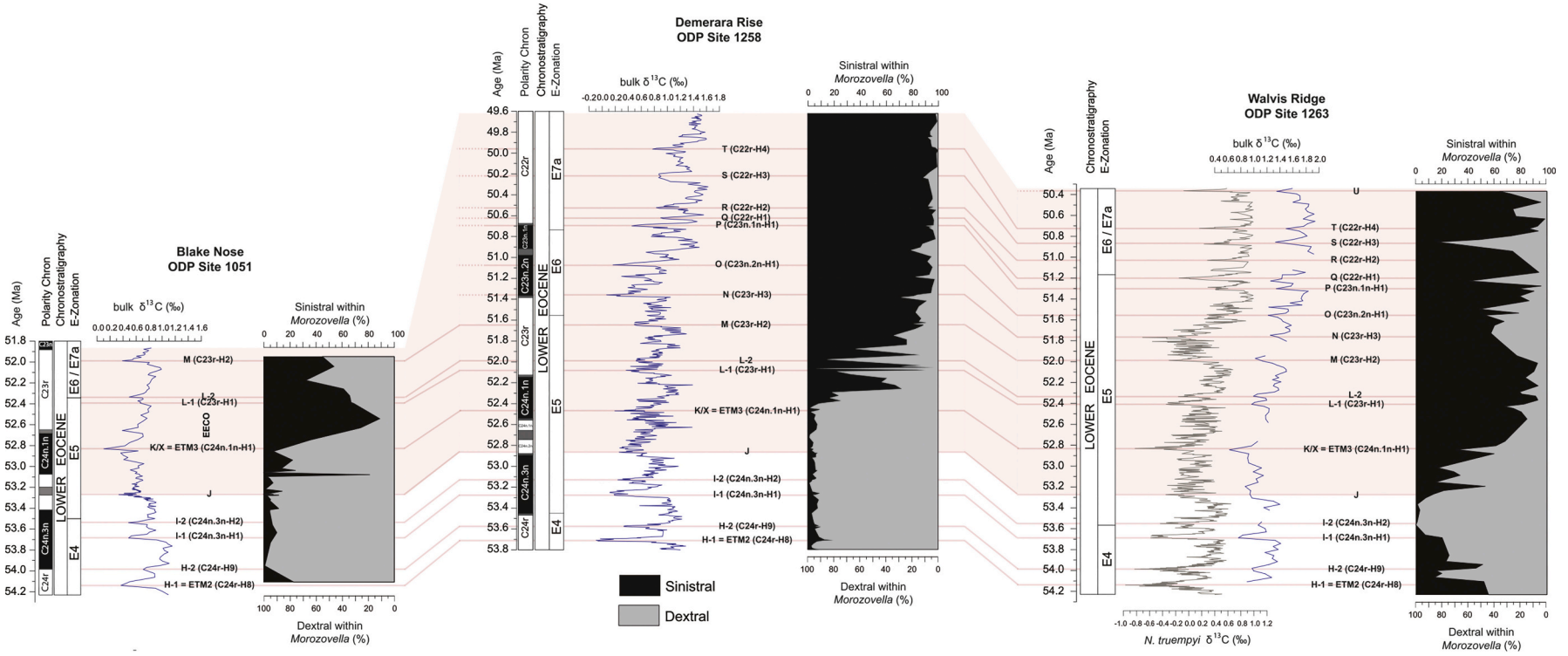

Fig. 8. Change in coiling direction of the genus *Morozovella* plotted in age from the sites 1051, 1258 and 1263. Note that the switch between dominantly DX to dominantly SN morphotypes occurred at the three sites within 200 kyr after the K/X event. These results can provide a new biostratigraphic tool for Eocene successions. Site 1051: Bulk $\delta^{13}C$ curve is from Luciani et al. (2017a). Site 1258: bulk $\delta^{13}C$ curve is from Kirtland-Turner et al., 2014). Site 1263: the $\delta^{13}C$ record from benthic foraminifera (*N. truempyi*) comes from Lauretano et al. (2016) (grey) and the bulk sediment $\delta^{13}C$ curve is from Luciani et al. (2017b). The main carbon isotope excursions are labelled according to Westerhold et al. (2018).

Table 1
Depth (mbsf, rmcd), age (Ma) and kyr with respect to the J event and K/X events of the morozovellid permanent abundance decline (which occurred close the J event) and change from dominant dextral to sinistral coiling (which occurred after the K/X event) at the Atlantic sites 1051, 1258 and 1263. Chron are also added. (where available). The ages estimated for the J and K/X events are 52.831 Ma and 53.270 Ma respectively according to Lauretano et al. (2016), 52.818 Ma and 52.478 Ma respectively according to Kirtland-Turner et al. (2014). Note that morozovellids first declined permanently in abundance at the equatorial Site 1258 then extended at higher latitudes and that the morozovellid coiling direction change from dominantly dextral to dominantly sinistral occurred <~200 kyr after the K/X event.

	Morozovellid	Depth	Age	Chron
Site 1051	Abundance decline	428.2 mbsf	53.265 Ma (Lauretano et al., 2016) 0 = J event	Base C24n.2n
	Main coiling change	413.8 mbsf	52.626 Ma (Lauretano et al., 2016) +205 kyr after K/X event	C24n.1n
Site 1258	Abundance decline	107.87 rmcd	52.894 Ma (Kirtland-Turner et al., 2014) −20 kyr before J event	Top C24n.3n
	Main coiling change	102.12 rmcd	52.273 Ma (Kirtland-Turner et al., 2014) +206 kyr after K/X event	C24n.1n
Site 1263	Abundance decline	277.643 rmcd	53.105 Ma (Lauretano et al., 2016) +165 kyr after J event	//
	Main coiling change	273.12 rmcd	52.678 Ma (Lauretano et al., 2016) +153 kyr after K/X event	//

with independent stratigraphy to verify whether such changes can be detected elsewhere. This might include re-examination of previous sites that seem to show morozovellid coiling switches in the early Eocene (Bolli, 1950; Luterbacher, 1964; Pearson, 1993; Norris and Nishi, 2001), and other locations where the abundance "crash" in morozovellids occurred.

8. Summary and conclusions

Our records provide new insights on the relationship between early Eocene carbon-cycle changes and the relative abundance and coiling direction of the trochospiral planktic foraminiferal genus *Morozovella*. We investigated the coiling direction within *Morozovella* populations from sections at three widely separated locations in the Atlantic Ocean ODP sites 1051, 1258 and 1263, which span the EECO (~49–53 Ma), the interval when Earth surface temperatures and atmospheric pCO_2 very likely reached their Cenozoic maximum (e.g., Zachos et al., 2001, 2008; Anagnostou et al., 2016; Inglis et al., 2020). The symbiont-bearing surface-dweller planktic foraminiferal genus *Morozovella* was a clear target because it dominated tropical-subtropical early Paleogene assemblages, but its abundance abruptly and permanently declined across the carbon isotope excursion known as the J event, which marks the beginning of the EECO (Luciani et al., 2016, 2017a, 2017b; D'Onofrio et al., 2020).

Our results demonstrate that multiple species of *Morozovella* display a dominant DX preference during the interval preceding the EECO at all sites. However, all species existing at the time show prominent SN coiling mode that became permanent within ~200 kyr after the K/X event. Temporary but significant switches towards sinistrally coiled morphotypes also occurred at sites 1051 and 1258 during some pre-EECO hyperthermals. The dominance of SN coiling during times of extreme warmth, whether the relatively long-term EECO or relatively short-term hyperthermals, strongly suggest a causal relationship to environment and possibly to temperature increase, although other conditions likely changed in concert with very warm surface waters. The remarkable variations in the coiling mode of *Morozovella* during extreme warming intervals of the early Paleogene shed new light on coiling direction preferences of planktic foraminifera. Morphologically defined species existing during the early Eocene show different coiling mode much more oftenly than previously thought (Norris and Nishi, 2001).

Our new stable isotope data, collected from SN and DX morphotypes at different time intervals below and above the major coiling shift, provide information on the habitat and/or ecological behaviour of the two morphotypes. Specifically, most of the sinistrally coiled morphospecies have lighter $\delta^{13}C$ values. This may imply that they lived slightly deeper than DX forms within the mixed-layer or, more likely, that SN morphotypes had reduced photosymbiotic relationships, both below and above the major coiling shift, with respect to DX morphotypes. Our data suggest indeed that the reduced photosymbiotic relationships of SN morphotypes, possibly taking advantage by a slightly deeper position within the mixed-layer enabled them to better tolerate water stressors occurring during the EECO. It is thus possible that only SN coiled morphotypes had enough flexibility to keep the optimal environmental conditions for their survivorship across the EECO. We can hypothesize that chemical and physical parameters within the mixed-layer, including temperature, food availability, pH reduction, excess of ultraviolet light, may have changed at the onset of the EECO. In the genetically controlled scenario, cryptic species with SN coiling were more resilient to environmental conditions across the start of the EECO than cryptic species with DX coiling.

The end-member alternative is that observed coiling changes were exclusively ecophenotypic responses whereby different species were able to preferentially adopt SN coiling to adapt to conditions that persisted in the mixed-layer conditions during the EECO. Previous interpretations of coiling flips in planktic foraminifera in the early Eocene, especially including morozovellids, have favoured a genetic explanation rather than an ecological response (e.g., Norris and Nishi, 2001). Our present data cannot validate or disprove this idea, but should stimulate renewed thought on the matter.

We need more effort to understand the meaning of these modifications, including a comprehensive knowledge of the EECO in terms of environmental change in surface waters during this time. Despite being the most prominent long-term interval of global warmth during the Cenozoic, detailed records remain scarce. Our data highlight that the recorded coiling variations might provide a new biostratigraphic tool for correlation of early Eocene marine strata and should motivate further high-resolution studies elsewhere.

Declaration of Competing Interest

I declare that there is no conflict of interest.

Acknowledgments

We warmly thank two anonymous reviewers and Editor Fabienne Marret-Davies for the constructive comments. Data supporting this paper are available as in Tables S1–S3 in the supplementary information. Funding for this research was provided for V.L. and R.D'O. by the Cofinanziamento MIUR (Italian Ministero dell'Istruzione, dell'Università e Ricerca) P.R.I.N. (Progetti di Ricerca di interesse nazionale to V. LUCIANI (within a National Research Project coordinated by E. Erba, Milan University, Italy, P.R.I.N. 2017, 2017RX9XXXY "Biota resilience

to global change: biomineralization of planktic and benthic calcifiers in the past, present and future" and by the Ferrara University (FAR –Fondo Ateneo Ricerca- Luciani 2016 and 2017). G.D. was financially supported by the U.S. National Science Foundation (grant NSF-FESD-OCE-1338842), and B.W. was supported by UK Natural Environment Research Council (NERC) reference number NE/G014817. Samples were provided by the International Ocean Discovery Program (IODP). IODP is sponsored by the U.S. National Science Foundation and participating countries. We thank the Bremen Core Repository for handling our sample request. SEM images were acquired at the Centro di Microscopia Elettronica of the Ferrara University.

Appendix A. Taxonomic list of planktic foraminiferal and calcareous nannofossil species cited in text and figures

Acarinina cuneicamerata (Blow, 1979).
Astrorotalia palmerae (Cushman and Bermúdez, 1937)
Globanomalina pseudomenardii (Bolli, 1957)
Globigerina bulloides d'Orbigny, 1826
Globigerinoides ruber (d'Orbigny, 1839)
Globorotalia truncatulinoides (d'Orbigny, 1839)
Igorina albeari Cushman and Bermudez, 1949
Morozovella aequa (Cushman and Renz, 1942)
Morozovella aragonensis (Nuttall, 1930)
Morozovella caucasica (Glaessner, 1937)
Morozovella crater (Hornibrook, 1958)
Morozovella gracilis (Bolli, 1957)
Morozovella lensiformis (Subbotina, 1953)
Morozovella marginodentata (Subbotina, 1953)
Morozovella subbotinae (Morozova, 1939)
Morozovella velascoensis (Cushman, 1925)
Neogloboquadrina acostaensis (Blow, 1959)
Neogloboquadrina pachyderma (Ehrenberg, 1861)
Neogloboquadrina incompta (Cifelli, 1961)
Rotalipora cushmani (Morrow, 1934)
Coccolithus pelagicus (Wallich) J.Schiller 1930
Heliolithus kleinpelli Sullivan, 1964

Appendix B. Supplementary data

Supplementary data to this article can be found online at https://doi.org/10.1016/j.gloplacha.2021.103634

References

Agnini, C., Backman, J., Brinkhuis, H., Fornaciari, E., Giusberti, L., Luciani, V., Rio, D., Sluijs, A., 2009. An early Eocene carbon cycle perturbation at similar to 52.5 Ma in the Southern Alps: Chronology and biotic response. Paleoceanography 24, PA2209. https://doi.org/10.1029/2008PA001649.

Anagnostou, E.H.J., Edgar, K.M., Foster, G.L., Ridgwell, A., Inglis, G.N., Pancost, R.D., Lunt, D.J., Pearson, P.N., 2016. Changing atmospheric CO2 concentration was the primary driver of early Cenozoic climate. Nature 533, 380–384. https://doi.org/10.1038/nature17423.

Aurahs, R., Grimm, G.W., Hemleben, V., Hemleben, C., Kucera, M., 2009. Geographical distribution of cryptic genetic types in the planktonic foraminifer *Globigerinoides ruber*. Mol. Ecol. 18 (8), 1692–1706.

Aze, T., Ezard, T.H.G., Purvis, A., Coxall, H.K., Stewart, D.R.M., Wade, B.S., Pearson, P. N., 2011. A phylogeny of Cenozoic macroperforate planktonic foraminifera from fossil data. Biol. Rev. 86, 900–927. https://doi.org/10.1111/j.1469-185X.2011.00178.x.

Bandy, O.L., 1960. The geologic significance of coiling ratios in the foraminifer *Globigerina pachyderma* (Ehrenberg). J. Paleontol. 34, 671–681.

Bandy, O.L., 1972. Origin and development of *Globorotalia* (*Turborotalia*) *pachyderma* (Ehrenberg). Micropaleontology 18, 294–318.

Bauch, D., Darling, K., Simstich, J., Bauch, H.A., Erlenkeuser, H., Kroon, D., 2003. Palaeoceanographic implications of genetic variation in living North Atlantic *N. pachyderma*. Nature 424, 299–302.

Be, A.W.H., Spero, H.J., Anderson, O.R., 1982. Effects of symbiont elimination and reinfection on the life processes of the planktonic foraminifer Globigerinoides sacculifer. Mar. Biol. 70, 73–86.

Berggren, W.A., Kent, D.V., Swisher III, C.C., Aubry, M.-P., 1995. A revised Cenozoic geochronology and chronostratigraphy. In: Berggren, W.A., Kent, D.V., Aubry, M.-P., Hardenbol, J. (Eds.), Geochronology, Time Scales and Global Stratigraphic Correlation, SEPM (Society for Sedimentary Geology Special Publication), vol. 54, pp. 129–212.

Bijl, P.K., Schouten, S., Sluijs, A., Reichart, G.-J., Zachos, J.C., Brinkhuis, H., 2009. Early Paleogene temperature evolution of the Southwest Pacific Ocean. Nature 461, 776–779. https://doi.org/10.1038/nature08399.

Billups, K., Vizcaino, M., Chiarello, J., Kaiser, E.A., 2020. Reconstructing Western boundary current stability in the North Atlantic Ocean for the past 700 Kyr from *Globorotalia truncatulinoides* coiling ratios. Paleoceanogr. Paleocleimatol. 35 (2), e2020PA003958 https://doi.org/10.1029/2020PA003958.

Boersma, A., Premoli Silva, I., 1983. Paleocene planktonic foraminiferal biogeography and the paleoceanography of the Atlantic-Ocean. Micropaleontology 29, 355–381.

Boersma, A., Premoli Silva, I., Shackleton, N., 1987. Atlantic Eocene planktonic foraminiferal biogeography and stable isotopic paleoceanography. Paleoceanography 2, 287–331.

Bohaty, S.M., Zachos, J.C., Florindo, F.M., Delaney, L., 2009. Coupled greenhouse warming and deep-sea acidification in the middle Eocene. Paleoceanography 24 (2). Doi:https://doi.org/10.1029/2008PA001676.

Bolli, H.M., 1950. The direction of coiling in the evolution of some *Globorotaliidae*. Contrib. Cushman Found. Foraminiferal Res. 1, 82–89.

Bolli, H.M., 1971. The direction of coiling in planktonic foraminifera. In: Funnell, B.M., Riedel, W.R. (Eds.), The Micropaleontology of Oceans. Cambridge University Press, Cambridge, United Kingdom, pp. 639–648.

Boltovoskoy, E., Wright, R., 1976. In: Junk, W. (Ed.), Recent Foraminifera. The Hague, p. 515. https://doi.org/10.1007/978-94-017-2860-7.

Bond, G., Broecker, W., Johnsen, S., McManus, J., Labeyrie, L., Jouzel, J., Bonani, G., 1993. Correlations between climate records from North Atlantic sediments and Greenland ice. Nature 365 (6442), 143–147.

Caron, M., 1981. Un nouveau genre de foraminifère planctonique du Crétacé: *Falsotruncana* nov. gen. Eclogae Geol. Helv. 74, 65–73.

Cifelli, R., 1961. *Globigerina incompta*, a new species of pelagic foraminifera from the North Atlantic. Contrib. Cushman Lab. Foram. Res. 12, 83–86.

Coccioni, R., Bancalà, G., Catanzariti, R., Fornaciari, E., Frontalini, F., Giusberti, L., Jovane, L., Luciani, V., Savian, J., Sprovieri, M., 2012. An integrated stratigraphic record of the Palaeocene-lower Eocene at Gubbio (Italy), New insights into the early Palaeogene hyperthermals and carbon isotope excursions. Terra Nova 24, 380–386. https://doi.org/10.1111/j.1365-3121.2012.01076.x.

Coccioni, R., Sideri, M., Frontalini, F., Montanari, A., 2016. The *Rotalipora cushmani* extinction at Gubbio (Italy): Planktonic foraminiferal testimonial of the onset of the Caribbean large igneous province emplacement? Geol. Soc. Am. Spec. 524, 81–96.

Cramer, B.S., Kent, D.V., Aubry, M.-P., 2003. Orbital climate forcing of excursions in the late Paleocene–early Eocene (chrons C24n–C25n). Paleoceanography 18 (4), 1097. https://doi.org/10.1029/2003PA000909.

Darling, K.F., Kucera, M.C., Wade, C.M., von Langen, P., Pak, D., 2003. Seasonal distribution of genetic types of planktonic foraminifer morphospecies in the Santa Barbara Channel and its paleoceanographic implications. Paleoceanography 18 (2), 1032. https://doi.org/10.1029/2001PA000723.

Darling, K.F., Kucera, M.C., Pudsey, C.J., Wade, C.M., 2004. Molecular evidence links cryptic diversification in polar plankton to Quaternary climate dynamic. PNAS 101, 7657–7662.

Darling, K.F., Kucera, M., Kroon, D., Wade, C.M., 2006. A resolution for the coiling direction paradox in *Neogloboquadrina pachyderma*. Paleoceanography, PA2011. https://doi.org/10.1029/2005PA001189.1.

Davis, C.V., Livsey, C.M., Palmer, H.M., Pincelli, M.H., Thomas, E., Hill, T.M., Benitez-Nelson, C.R., 2020. Extensive morphological variability in asexually produced planktic foraminifera. Sci. Adv. 6 (28), eabb8930 https://doi.org/10.1126/sciadv.abb8930.

Dedert, M., Stoll, H.M., Kroon, D., Shimizu, N., Kanamaru, K., Ziveri, P., 2012. Productivity response of calcareous nannoplankton to Eocene thermal Maximum 2 (ETM2). Clim. Past 8 (3), 977–993. https://doi.org/10.5194/cp-8-977-2012.

Dedert, M., Stoll, H.M., Kars, S., Young, J.R., Shimizu, N., Kroon, D., Lourens, L., Ziveri, P., 2014. Temporally variable diagenetic overgrowth on deep-sea nannofossil carbonates across Palaeogene hyperthermals and implications for isotopic analyses. Mar. Micropaleontol. 107, 18–31. https://doi.org/10.1016/j. marmicro.2013.12.

Desmares, D., Crognier, N., Bardin, J., Testé, M., Beaudoin, B., Grosheny, D., 2016. A new proxy for cretaceous paleoceanographic and paleoclimatic reconstructions: Coiling direction changes in the planktonic foraminifera *Muricohedbergella delrioensis*. Palaeogeogr. Palaeoclimatol. Palaeoecol. 445, 8–17.

D'Haenens, S., Bornemann, A., Claeys, P., Röhl, U., Steurbaut, E., Speijer, R.P., 2014. A transient deep-sea circulation switch during Eocene thermal Maximum 2. Paleoceanography 29, 370–388. https://doi.org/10.1002/2013PA002567.

D'Onofrio, R., Luciani, V., Giusberti, L., Fornaciari, E., Sprovieri, M., 2014. Tethyan planktic foraminiferal record of the early Eocene hyperthermal events ETM2, H2 and I1 (Terche section, northeastern Italy). Rendiconti Online Soc. Geol. It. 31, 66–67. https://doi.org/10.3301/ROL.2014.48.

D'Onofrio, R., Luciani, V., Fornaciari, E., Giusberti, L., Boscolo Galazzo, F., Dallanave, E., Westerhold, T., Sprovieri, M., Telch, S., 2016. Environmental perturbations at the early Eocene ETM2, H2, and I1 events as inferred by Tethyan calcareous plankton (Terche section, northeastern Italy). Paleoceanography 31 (9), 1225–1247. https://doi.org/10.1002/2016PA002940.

D'Onofrio, R., Luciani, V., Dickens, G.R., Wade, B.S., Kirtland, Turner S., 2020. Demise of the Planktic Foraminifer Genus *Morozovella* during the Early Eocene climatic optimum: new records from ODP Site 1258 (Demerara Rise,Western Equatorial Atlantic) and site 1263 (Walvis Ridge, South Atlantic). Geosciences 10, 88. https://doi.org/10.3390/geosciences10030088.

Edgar, K.M., Pälike, H., Wilson, P., 2013. Testing the impact of diagenesis on the $\delta^{18}O$ and $\delta^{13}C$ of benthic foraminiferal calcite from a sediment burial depth transect in the equatorial Pacific. Paleoceanography 28 (3). https://doi.org/10.1002/palo.20045.

Edgar, K.M., Anagnostou, E., Pearson, P.N., Foster, G.L., 2015. Assessing the impact of diagenesis on $\delta^{11}B$, $\delta^{13}C$, $\delta^{18}O$, Sr/Ca and B/Ca values in fossil planktic foraminiferal calcite. Geochim. Cosmochim. Acta 166, 189–209. https://doi.org/10.1016/j.gca.2015.06.018.

Ericson, D.B., 1959. Coiling direction of *Globigerina pachyderma* as a climatic index. Science 130, 219–220.

Ericson, D.B., Wollin, G., Wollin, J., 1955. Coiling direction of *Globorotalia truncatulinoides* in deep-sea cores. Deep Sea Res. (1953) 2 (2), 152–158. https://doi.org/10.1016/0146-6313(55)90018-6. IN7.

Ezard, T.H.G., Aze, T., Pearson, P.N., Purvis, A., 2011. Interplay between changing climate and species ecology drives macroevolutionary dynamics. Science 332, 349–351. https://doi.org/10.1126/science.1203060.

Feldmeijer, W., Metcalfe, B., Brummer, G.-J.A., Ganssen, G.M., 2015. Reconstructing the depth of the permanent thermocline through the morphology and geochemistry of the deep dwelling planktonic foraminifer *Globorotalia truncatulinoides*. Paleoceanography 30, 1–22. https://doi.org/10.1002/2014PA002687.

Fraass, A.J., Kelly, D.K., Peters, S.E., 2015. Macroevolutionary history of the planktic foraminifera. Annu. Rev. Earth Pl. Sc. 43, 139–166. https://doi.org/10.1146/annurev-earth-060614-105059.

Frank, T.D., Arthur, M.A., Dean, W.E., 1999. Diagenesis of lower cretaceous pelagic carbonates, North Atlantic: paleo- ceanographic signals obscured. J. Foramin. Res. 29, 340–351.

Frontalini, F., Coccioni, R., Catanzariti, R., Jovane, L., Savian, J.F., Sprovieri, M., 2016. The Eocene thermal maximum 3: reading the environmental perturbations at Gubbio (Italy). Geol. Soc. Am. Spec. 524, SPE524–11.

Gaskell, Daniel E., Hull, Pincelli M., 2019. Symbiont arrangement and metabolism can explain high δ13C in Eocene planktonic foraminifera. Geology 47-12 (1156–1160).

Gibbs, S.J., Bown, P.R., Murphy, B.H., Sluijs, A., Edgar, K.M., Pälike, H., Bolton, C.T., Zachos, J.C., 2012. Scaled biotic disruption during early Eocene global warming events. Biogeosciences 9 (11), 4679–4688. https://doi.org/10.5194/bg-9-4679-2012.

Green, O.R., 2001. A Manual of Practical Laboratory and Field Techniques in Palaeobiology. Kluwer Academic, London.

Grosheny, D., Ferry, S., Lécuyer, C., Thomas, A., Desmares, D., 2017. The Cenomanian-Turonian Boundary Event (CTBE) on the southern slope of the Subalpine Basin (SE France) and its bearing on a probable tectonic pulse on a larger scale. Cretac. Res. 72, 39–65.

Hallock, P., 1987. Fluctuations in the trophic resource continuum: a factor in global diversity cycles? Paleoceanography 2, 457–471.

Hancock, H.J.L., 2005. Coiling shifts and stable isotope changes in the late Paleocene planktic foraminifera *Igorina albeari*: expression and significance. In: Early Paleogene planktic foraminiferal assemblages in Australasian sequences: Link to Past Changes in Climate and Carbon Cycling. PhD Thesis. James Cook University, North Queensland, Australia.

Hemleben, C., 1989. In: Spindler, M., Anderson, O.R. (Eds.), Modern Planktonic Foraminifera. Springer-Verlag, 363 pp.

Hodell, D.A., Benson, R.H., Kent, D.V., Boersma, A., Bied, R.E., 1994. Magnetostratigraphic, biostratigraphic, and stable isotope stratigraphy of an Upper Miocene drill core from the Salé Briqueterie (northwestern Morocco): a high-resolution chronology for the Messinian stage. Paleoceanography 9 (6), 835–855.

Hodell, D.A., Curtis, J.H., Sierro, F.J., Raymo, M.E., 2001. Correlation of late Miocene to early Pliocene sequences between the Mediterranean and North Atlantic. Paleoceanography 16 (2), 164–178.

Hollis, C.J., Taylor, K.W.R., Handley, L., Pancost, R.D., Huber, M., Creech, J.B., Hines, B. R., Crouch, E.M., Morgans, H.E.G., Crampton, J.S., Gibbs, S., Pearson, P., Zachos, J. C., 2012. Early Paleogene temperature history of the Southwest Pacific Ocean: Reconciling proxies and models. Earth Planet. Sci. Lett. 374, 258–259. https://doi.org/10.1016/j.epsl.2013.06.012.

Hollis, C.J., Dunkley Jones, T., Anagnostou, E., Bijl, P.K., Cramwinckel, M.J., Cui, Y., Dickens, G.R., Edgar, K.M., Eley, Y., Evans, D., Foster, G.L., Frieling, J., Inglis, G.N., Kennedy, E.M., Kozdon, R., Lauretano, V., Lear, C.H., Littler, K., Lourens, L., Meckler, A.N., Naafs, B.D.A., Pälike, H., Pancost, R.D., Pearson, P.N., Röhl, U., Royer, D.L., Salzmann, U., Schubert, B.A., Seebeck, H., Sluijs, A., Speijer, R.P., Stassen, P., Tierney, J., Tripati, A., Wade, B., Westerhold, T., Witkowski, C., Zachos, J.C., Zhang, Y.G., Huber, M., Lunt, D.J., 2019. The DeepMIP contribution to PMIP4: methodologies for selection, compilation and analysis of latest Paleocene and early Eocene climate proxy data, incorporating version 0.1 of the DeepMIP database. Geosci. Model Dev. 12, 3149–3206. https://doi.org/10.5194/gmd-12-3149-2019.

Hooper, P.W.P., Weaver, P.P.E., 1987. Paleoceanographic significance of late Miocene to early Pliocene planktonic foraminifers at Deep-sea Drilling Project Site-609. DSDP Initial Reports 94, 925–934.

Huber, M., Caballero, R., 2011. The early Eocene equable climate problem revisited. Clim. Past 7, 603–633. https://doi.org/10.5194/cp-7-603-2011.

Inglis, G.N., Farnsworth, A., Lunt, D., Foster, G.L., Hollis, C.J., Pagani, M., Jardine, P.E., Pearson, P.N., Markwick, P., Galsworthy, A.M.J., Raynham, L., Taylor, K.W.R., Pancost, R.D., 2015. Descent toward the icehouse: Eocene Sea surface cooling inferred from GDGT distributions. Paleoceanography 30, 1000–1020. https://doi.org/10.1002/2014PA002723.

Inglis, G.N., Bragg, F., Burls, N.J., Cramwinckel, M.J., Evans, D., Gavin, L., Foster, G.L., Huber, M., Lunt, D.J., Siler, N., Steinig, S., Tierney, J.E., Wilkinson, R., Anagnostou, E., de Boer, A.M., Dunkley Jones, T., Edgar, K.M., Hollis, C.J., Hutchinson, D.K., Pancost, R.D., 2020. Global mean surface temperature and climate sensitivity of the early Eocene Climatic Optimum (EECO), Paleocene–Eocene thermal Maximum (PETM), and latest Paleocene. Clim. Past 16, 1953–1968. https://doi.org/10.5194/cp-16-1953-2020.

John, E.H., Wilson, J.D., Pearson, P.N., Ridwell, A., 2013. Warm processes and carbon cycling in the Eocene. Philos. Trans. R. Soc. A Math. Phys. Eng. Sci. 371 (2001). Doi: https://doi.org/10.1098/rsta.2013.0099. Article number: 20130099.

John, E.H., Pearson, P.N., Coxall, H.K., Birch, H., Wade, B.S., Foster, G.L., 2014. Temperaure-dependent remineralizationand carbon cycling in the warm Eocene oceans. Palaeogeogr. Palaeoclimatol. Palaeoecol. 413, 158–166. https://doi.org/10.1016/j.palaeo.2014.05.019.

Keigwin, L.D., 1978. Pliocene closing of the Isthmus of Panama, based on biostratigraphic evidence from nearby Pacific Ocean and Caribbean Sea cores. Geology 6 (10), 630–634.

Khare, N., Mazumder, A., Govil, P., 2012. Do changes in coiling directions in planktonic foraminifera correspond to dimorphic reproduction? Oceanology 52, 364–371. https://doi.org/10.1134/S0001437012030058.

Kim, J.-H., van der Meer, J., Schouten, S., Helmke, P., Willmott, V., Sangiorgi, F., Koç, N., Hopmans, E.C., Damsté, J.S.S., 2010. New indices and calibrations derived from the distribution of crenarchaeal isoprenoid tetraether lipids: implications for past sea surface temperature reconstructions Geochim. Cosmochim. Acta 74, 4639–4654. https://doi.org/10.1016/j.gca.2010.05.027.

Kimoto, K., Tsuchiya, M., 2006. The "unusual" reproduction of planktic foraminifera: an asexual reproductive phase of *Neogloboquadrina pachyderma* (Ehrenberg). In: Abstract Volume, International Symposium on Foraminifera (FORAMS 2006). Anuário do Instituto de Geociências– UFRJ 29: 461.

Kirtland-Turner, S., Sexton, P.F., Charles, C.D., Norris, R.D., 2014. Persistence of carbon release events through the peak of early Eocene global warmth. Nat. Geosci. 12, 1–17. https://doi.org/10.1038/ngeo2240.

Kucera, M., Kennett, J.P., 2002. Causes and consequences of a middle Pleistocene origin of the modern planktonic foraminifer *Neogloboquadrina pachyderma* sinistral. Geology 30 (6), 539–542.

Lauretano, V., Littler, K., Polling, M., Zachos, J.C., Lourens, L.J., 2015. Frequency, magnitude and character of hyperthermal events at the onset of the early Eocene Climatic Optimum. Clim. Past 11, 1313–1324. https://doi.org/10.5194/cp-11-1313-2015.

Lauretano, V., Hilgen, F.J., Zachos, J.C., Lourens, L.J., 2016. Astronomically tuned age model for the early Eocene carbon isotope events: a new high-resolution $\delta^{13}C$ benthic record of ODP Site 1263 between~ 49 and~ 54 Ma. Newsl. Stratigr. 49 (2), 383–400.

Leon-Rodriguez, L., Dickens, G.R., 2010. Constraints on ocean acidification associated with rapid and massive carbon injections: the early Paleogene record at ocean drilling program site 1215, equatorial Pacific Ocean. Palaeogeogr. Palaeoclimatol. Palaeoecol. 298 (3–4), 409–420. https://doi.org/10.1016/j.palaeo.2010.10.029.

Littler, K., Röhl, U., Westerhold, T., Zachos, J.C., 2014. A high-resolution benthic stable isotope record for the South Atlantic: Implications for orbital-scale changes in late Paleocene–early Eocene climate and carbon cycling. Earth Planet. Sci. Lett. 401, 18–30. https://doi.org/10.1016/j.epsl.2014.05.054.

Liu, Z., Pagani, M., Zinniker, D., DeConto, R., Huber, M., Brinkhuis, H., Sunita, R.S., Leckie, R.M., Pearson, P.N., 2009. Global cooling during the Eocene-Oligocene climate transition. Science 323 (5918), 1187–1190. https://doi.org/10.1126/science.1166368.

Lourens, L.J., Sluijs, A., Kroon, D., Zachos, J.C., Thomas, E., Röhl, U., Bowles, J., Raffi, I., 2005. Astronomical pacing of late Palaeocene to early Eocene global warming events. Nature 435, 1083–1087. https://doi.org/10.1038/nature03814.

Luciani, V., Giusberti, L., 2014. Reassessment of the early–middle Eocene planktic foraminiferal biomagnetochronology: new evidence from the Tethyan Possagno section (NE Italy) and Western North Atlantic Ocean ODP Site 1051. J. Foram. Res. 44, 187–201.

Luciani, V., Dickens, G.R., Backman, J., Fornaciari, E., Giusberti, L., Agnini, C., D'Onofrio, R., 2016. Major perturbations in the global carbon cycle and photosymbiont-bearing planktic foraminifera during the early Eocene. Clim. Past 12, 981–1007. https://doi.org/10.5194/cp-12-981-2016.

Luciani, V., D'Onofrio, R., Dickens, G.R., Wade, B.S., 2017a. Did photosymbiont bleaching lead to the demise of planktic foraminifer *Morozovella* at the early Eocene Climatic Optimum? Paleoceanography 32, 1115–1136. https://doi.org/10.1002/2017PA003138.

Luciani, V., D'Onofrio, R., Dickens, G.R., Wade, B.S., 2017b. Planktic foraminiferal response to early Eocene carbon cycle perturbations in the Southeast Atlantic Ocean (ODP Site 1263). Glob. Planet. Chang. 158, 119–133. https://doi.org/10.1016/j.gloplacha.2017.09.007.

Luterbacher, H., 1964. Studies in some *Globorotalia* from the Paleocene and lower Eocene of the Central Apennines. Eclogae Geol. Helv. 57, 631–730.

Malmgren, B.A., 1989. Coiling patterns in terminal cretaceous planktonic foraminifera. J. Foram. Res. 19, 311–323.

Martinez, J.I., Mora, G., Barrows, T.T., 2007. Paleoceanographic conditions in the Western Caribbean Sea for the last 560 Kyr as inferred from planktonic foraminifera. Mar. Micropaleontol. 64, 177–188. https://doi.org/10.1016/j.marmicro.2007.04.004.

Mita, I., 2001. Data Report: early to late Eocene calcareous nannofossil assemblages of Sites 1051 and 1052, Blake Nose, Northwestern Atlantic Ocean. In: Kroon, D., Norris, R.D., Klaus, A. (Eds.), Proceedings of the Ocean Drilling Program Scientific Results, 171B, pp. 1–28. World Wide Web. Available from. http://wwwodp.tamu.edu/publications/171B_SR/chap_07/chap_07.htm>.

Morard, R., Reinelt, M., Chiessi, C.M., Groeneveld, J., Kucera, M., 2016. Tracing shifts of oceanic fronts using the cryptic diversity of the planktonic foraminifera *Globorotalia inflate*. Paleoceanography 31 (9), 1193–1205.

Nicolo, M.J., Dickens, G.R., Hollis, C.J., Zachos, J.C., 2007. Multiple early Eocene hyperthermals: their sedimentary expression on the New Zealand continental margin and in the deep sea. Geology 35 (8), 699–702. https://doi.org/10.1130/G23648A.1.
Norris, R.D., 1991. Biased extinction and evolutionary trends. Paleobiology 17, 388–399.
Norris, R.D., Nishi, H., 2001. Evolutionary trends in coiling of tropical Paleogene planktic foraminifera. Paleobiology 27, 327–347.
Norris, R.D., Kroon, D., Klaus, A., 1998. Blake Nose paleoceanographic transect, Western North Atlantic. Proceedings of the Ocean Drilling Program, initial reports. Proc. Ocean Drill. Program Sci. Results 171B, 1–749. https://doi.org/10.2973/odp.proc.ir.171b.1998.
Ogg, J.G., Bardot, L., 2001. Aptian through Eocene magnetostratigraphic correlation of the Blake Nose Transect (Leg 171B), Florida continental margin. Proc. Ocean Drill. Program Sci. Results 171B, 1–58. https://doi.org/10.2973/odp.proc.sr.171B.104.2001.
Olsson, R.K., Hemleben, C., Berggren, W.A., Huber, B.T., 1999. Atlas of Paleocene Planktonic Foraminifera. In: Smithsonian Contribution to Paleobiology 85. D. C., Smithsonian Institution Press, Washington. https://doi.org/10.5479/si.00810266.85.1.
Pearson, P.N., 1993. A Lineage Phylogeny for the Paleogene Planktonic Foraminifera. Micropaleontology 39 (3), 193–232. http://www.jstor.org/stable/1485898.
Pearson, P.N., Penny, L., 2021. Coiling directions in the planktonic foraminifer *Pulleniatina*: a complex eco- evolutionary dynamic spanning millions of years. PLoS One 16 (4), e0249113. https://doi.org/10.1371/journal.pone.0249113.
Pearson, P.N., Shackleton, N.J., Hall, M.A., 1993. Stable isotope paleoecology of middle Eocene planktonic foraminifera and multispecies isotope stratigraphy, DSDP Site 523, South Atlantic. J. Foraminifer. Res. 23, 123–140.
Pearson, P.N., Ditchfield, P.W., Singano, J., Harcourt-Brown, K.G., Nicholas, C.J., Olsson, R.K., Shackleton, N.J., Hall, M.A., 2001. Warm tropical sea surface temperatures in the late cretaceous and Eocene epochs. Nature 413, 481–487. https://doi.org/10.1038/35097000.
Pearson, P.N., Olsson, R.K., Hemblen, C., Huber, B.T., Berggren, W.A. (Eds.), 2006. Atlas of Eocene Planktonic Foraminifera, Cushman Special Publication, 41. Department of Geology East Carolina Univ, Greenville, p. 513.
Premoli Silva, I., Boersma, A., 1988. Atlantic Eocene planktonic foraminiferal historical biogeography and paleohydrographic indices. Palaeogeogr. Palaeoclimatol. Palaeoecol. 67 (3–4), 315–356. https://doi.org/10.1016/0031-0182(88)90159-9.
Pross, J., Contreras, L., Bijl, P.K., Greenwood, D.R., Bohaty, S.M., Schouten, S., Bendle, J. A., Röhl, U., Tauxe, L., Raine, J.I., Claire, E., Huck, C.E., van de Flierdt, T., Stewart, S.R., Jamieson, S.S.R., Stickley, C.E., van de Schootbrugge, B., Escutia, C., Brinkhuis, H., 2012. Persistent near-tropical warmth on the Antarctic continent during the early Eocene Epoch. Nature 488, 73–77. https://doi.org/10.1038/nature11300.
Quillévéré, F., Norris, R.D., Moussa, I., Berggren, W.A., 2001. Role of photosymbiosis and biogeography in the diversification of early Paleogene acarininids (planktonic foraminifera). Paleobiology 27 (2), 311–326. https://doi.org/10.1666/0094837(2001)027<0311:ROPABI>2.0.CO;2.
Renaud, S., Schmidt, D.N., 2003. Habitat tracking as a response of the planktic foraminifer *Globorotalia truncatulinoides* to environmental fluctuations during the last 140 kyr. Mar. Micropaleontol. 49, 97–122. https://doi.org/10.1016/S0377-8398(03)00031-8.
Röhl, U., Norris, R.D., Ogg, J.G., 2003. XRF iron (Fe) counts of ODP Hole 171-1050A and 171-1051A. *PANGAEA*. https://doi.org/10.1594/PANGAEA.816488. Supplement to: Röhl, U et al. (2003): Cyclostratigraphy of upper Paleocene and late Eocene sediments at Blake Nose Site 1051 (western North Atlantic). In: Gingerich, P., Schmitz, B,. Thomas, E., Wing, S. (Eds.), Causes and Consequences of Globally Warm Climates in the Early Paleogene, Geological Society of America (GSA) Special Paper 369, 567–588, doi:10.1130/0-8137-2369-8.567.
Saito, T., 1976. Geologic significance of coiling direction in the planktonic foraminifera *Pulleniatina*. Geology 4, 305–309.
Schmidt, D.N., Renaud, S., Bollmann, J., Schiebel, R., Thierstein, H.R., 2004. Size distribution of Holocene planktic foraminifer assemblages: Biogeography, ecology and adaptation. Mar. Micropaleontol. 50 (3–4), 319–338. https://doi.org/10.1016/S0377-8398(03)00098-7.
Scott, G.H., 1974. Biometry of the Foraminiferal Shell. In: Hedley, R.H., Adams, C.G. (Eds.), Foraminifera. London Academic Press, United Kingdom, pp. 55–152.
Sen Gupta, B.K., 2002. In: Sen Gupta, B.K. (Ed.), Modern Foraminifera. Kluwer Academic Publishers, 371 pp. ISBN: 9781402005985.
Sexton, P.F., Wilson, P.A., Pearson, P.N., 2006. Microstructural and geochemical perspectives on planktic foraminiferal preservation: 'Glassy' versus 'Frosty'. Geochem. Geophys. Geosyst. 7, Q12P19 https://doi.org/10.1029/2006GC001291.
Sexton, P.F., Norris, R.D., Wilson, P.A., Pälike, H., Westerhold, T., Röhl, U., Bolton, C.T., Gibbs, S.J., 2011. Eocene sedimentary calcium carbonate contents from ODP Sites 207-1258. PANGAEA. https://doi.org/10.1594/PANGAEA.763158. In supplement to: Sexton et al. (2011). Eocene global warming events driven by ventilation of oceanic dissolved organic carbon. Nature 471, 349-352. doi:10.1038/nature09826.
Shackleton, N.J., Corfield, R.M., Hall, M.A., 1985. Stable isotope data and the ontogeny of Paleocene planktonic foraminifera. J. Foram. Res. 15 (4), 321–336.
Shipboard Scientific Party, 1998. Site 1051. In: Norris, R.D. (Ed.), Proc. ODP, Init. Repts., 171B. Ocean Drilling Program, College Station, TX, pp. 171–239. https://doi.org/10.2973/odp.proc.ir.171b.105.1998.
Shipboard Scientific Party, 2004. Site 1258. In: Erbacher, J. (Ed.), Proceedings of the Ocean Drilling Program, Initial Reports. 207. Ocean Drilling Program, College Station, Texas, pp. 1–41.
Slotnick, B.S., Dickens, G.R., Nicolo, M.J., Hollis, C.J., Crampton, J.S., Zachos, J.C., 2012. Large-amplitude variations in carbon cycling and terrestrial weathering during the latest Paleocene and earliest Eocene: the record at Mead Stream. New Zealand J. Geol. Geophys. 120 (5), 487–505. https://doi.org/10.1086/666743.
Slotnick, B.S., Dickens, G.R., Hollis, C.J., Crampton, J.S., Strong, P.S., Phillips, A., 2015. The onset of the EarlyEocene Climatic Optimum at Branch Stream, Clarence Rivervalley, New Zealand. New Zealand J. Geol. Geophys. 58, 1–19. https://doi.org/10.1080/00288306.2015.1063514.
Spero, H.J., DeNiro, M.J., 1987. The influence of photosynthesis on the δ18O and δ13C values of planktonic foraminiferal shell calcite. Symbiosis 4, 213–228.
Stap, L., Sluijs, A., Thomas, E., Lourens, L.J., 2009. Patterns and magnitude of deep sea carbonate dissolution during Eocene thermal Maximum 2 and H2, Walvis Ridge, Southeastern Atlantic Ocean. Paleoceanography 24, PA1211. https://doi.org/10.1029/2008PA001655.
Stap, L., Lourens, L.J., Thomas, E., Sluijs, A., Bohaty, S., Zachos, J.C., 2010a. High-resolution deep-sea carbon and oxygen isotope records of Eocene thermal Maximum 2 and H2. Geology 38, 607–610. https://doi.org/10.1130/G30777.1.
Stap, L., Lourens, L.J., van Dijk, A., Schouten, S., Thomas, E., 2010b. Coherent pattern and timing of the carbon isotope excursion and warming during Eocene Thermal Maximum 2 as recorded in planktic and benthic foraminifera. Geochem. Geophys. Geosyst. 11, Q11011 https://doi.org/10.1029/2010GC003097.
Thomas, E., 1998. Biogeography of the late Paleocene benthic foraminiferal extinction. In: Aubry, M.-P., Lucas, S., Berggren, W.A. (Eds.), Late Paleocene–Early Eocene Climaticand Biotic Events in the Marine and Terrestrial Records. Columbia University Press, New York, United States of America, pp. 214–243.
Toumarkine, M., Luterbacher, H.P., 1985. Paleocene and Eocene planktonic foraminifera. In: Bolli, H.M., Saunders, J.B., Perch-Nielsen, K. (Eds.), Plankton Stratigraphy. Cambridge University Press, United Kingdom, pp. 87–154.
Tremolada, F., Bralower, T.J., 2004. Nannofossil assemblage fluctuations during the Paleocene-Eocene thermal maximum at Sites 213 (Indian Ocean) and 401 (North Atlantic Ocean): Palaeoceanographic implications. Mar. Micropaleontol. 52 (1), 107–116. https://doi.org/10.1016/j.marmicro.2004.04.002.
Ujiié, Y., Asami, T., 2014. Temperature is not responsible for left-right reversal in pelagic unicellular zooplanktons. J. Zool. 293 (1), 16–24.
Ujiié, Y., de Garidel-Thoron, T., Watanabe, S., Wiebe, P., de Vargas, C., 2010. Coiling dimorphism within a genetic type of the planktonic foraminifer *Globorotalia truncatulinoides*. Mar. Micropaleontol. 77 (3), 145–153.
Van Hinsbergen, D.J., de Groot, L.V., van Schaik, S.J., Spakman, W., Bijl, P.K., Sluijs, A., Langereis, C.G., Brinkhuis, H., 2015. A Paleolatitude Calculator for Paleoclimate Studies. PLoS One 10, e0126946. https://doi.org/10.1371/journal.pone.0126946.
Wade, B.S., Pearson, P.N., 2008. Planktonic foraminiferal turnover, diversity fluctuations and geochemical signals across the Eocene/Oligocene boundary in Tanzania. Mar. Micropaleontol. 68, 244–255. https://doi.org/10.1016/j.marmicro.2008.04.002.
Wade, B.S., Al-Sabouni, N., Hemleben, C., Kroon, D., 2008. Symbiont bleaching in fossil planktonic foraminifera. Evol. Ecol. 22, 253–265.
Wade, B.S., Pearson, P.N., Berggren, W.A., Pälike, H., 2011. Review and revision of Cenozoic tropical planktonic foraminiferal biostratigraphy and calibration to the geomagnetic polarity and astronomical time scale. Earth Sci. Rev. 104 (1–3), 111–142. https://doi.org/10.1016/j.earscirev.2010.09.003.
Westerhold, T., Röhl, U., Laskar, J., Raffi, I., Bowles, J., Lourens, L.J., Zachos, J.C., 2007. On the duration of magnetochrons C24r and C25n and the timing of early Eocene global warming events: implications from the Ocean Drilling Program Leg 208 Walvis Ridge depth transect. Paleoceanography 22, PA2201. https://doi.org/10.1029/2006PA001322.
Westerhold, T., Röhl, U., Laskar, J., 2012. Time scale controversy: Accurate orbital calibration of the early Paleogene. Geochem. Geophys. Geosyst. 13 https://doi.org/10.1029/2012GC004096.
Westerhold, T., Röhl, U., Frederichs, T., Bohaty, S.M., Zachos, J.C., 2015. Astronomical calibration of the geological timescale: closing the middle Eocene gap. Clim. Past 11 (9), 1181–1195. https://doi.org/10.5194/cp-11-1181-2015.
Westerhold, T., Röhl, U., Frederichs, T., Agnini, C., Raffi, I., Zachos, J.C., Wilkens, R.H., 2017. Astronomical calibration of the Ypresian timescale: implications for seafloor spreading rates and the chaotic behavior of the solar system? Clim. Past 13, 1129–1152. https://doi.org/10.5194/cp-13-1129-2017.
Westerhold, T., Röhl, U., Donner, B., Zachos, J.C., 2018. Global Extent of early Eocene Hyperthermal events: a New Pacific Benthic Foraminiferal Isotope RecordFrom Shatsky rise (ODP Site 1209). Paleoceanogr. Paleoclimatol. 33 https://doi.org/10.1029/2017PA003306.
Witkowski, J., Harwood, D.M., Wade, B.S., Brylka, K., 2020a. Rethinking the chronology of early Paleogene sediments in the western North Atlantic using diatom biostratigraphy. Mar. Geol. 424, 106168.
Witkowski, J., Penman, D.E., Bryłka, K., Wade, B.S., Matting, S., Harwood, D.M., Bohaty, S.M., 2020b. Early Paleogene biosiliceous sedimentation in the Atlantic Ocean: Testing the inorganic origin hypothesis for Paleocene and Eocene chert and porcellanite. Palaeogeogr. Palaeoclimatol. Palaeoecol. 556, 109896. https://doi.org/10.1016/j.palaeo.2020.109896.
Witkowski, J., Bryłka, K., Bohaty, S.M., Mydłowska, E., Penman, D.E., Wade, B.S., 2021. North Atlantic marine biogenic silica accumulation through the early-to-mid Paleogene: implications for ocean circulation and silicate weathering feedback. Clim. Past Discuss. https://doi.org/10.5194/cp-2021-50.
Xu, X., Kimoto, K., Oda, M., 1995. Predominance of left-coiling *Globorotalia truncatulinoides* (d'Orbigny) between 115.000 and 50.000 yrs. Quat. Res. 34 (1), 39–47.
Zachos, J.C., Pagani, M., Sloan, L., Thomas, E., Billups, K., 2001. Trends, rhythms, and aberrations in global climate 65 Ma to present. Science 292, 686–693. https://doi.org/10.1126/science.1059412.

Zachos, J.C., Kroon, D., Blum, P., et al., 2004. Proceedings of the Ocean Drilling Program initial reports 208. Ocean Drilling Program, College Station, TX. https://doi.org/10.2973/odp.proc.ir.208.2004.

Zachos, J.C., Röhl, U., Schellenberg, S.A., Sluijs, A., Hodell, H.A., Kelly, D.C., Thomas, E., Nicolo, M., Raffi, I., Lourens, L.J.H., Kroon, D., 2005. Rapid acidification of the ocean during the Paleocene-Eocene thermal maximum. Science 308, 1611–1615. https://doi.org/10.1126/science.1109004.

Zachos, J.C., Dickens, G.R., Zeebe, R.E., 2008. An early Cenozoic perspective on greenhouse warming and carbon-cycle dynamics. Nature 451 (7176), 279–283. https://doi.org/10.1038/nature06588.

Zachos, J.C., McCarren, H.K., Murphy, B., Röhl, U., Westerhold, T., 2010. Tempo and scale of late Paleocene and early Eocene carbon isotope cycles: Implications for the origin of hyperthermals. Earth Planet. Sci. Lett. 299, 242–249. https://doi.org/10.1016/j.epsl.2010.09.004.